Lindsie Jeffries
Department of Mechanical Engineering,
Stanford University,
Stanford, CA 94305
e-mail: lindsiej@stanford.edu

David Lentink
Department of Mechanical Engineering,
Stanford University,
Stanford, CA 94305
e-mail: dlentink@stanford.edu

Design Principles and Function of Mechanical Fasteners in Nature and Technology

Probabilistic mechanical fasteners are used to provide secure, reversible, and repeatable attachments in both nature and industry. Since the first observation of this mechanism in nature, which led to the creation of hook-and-loop fasteners, there has been a multitude of variations on the basic hook-and-loop design. However, few fastener designs have looked back to nature for inspiration in creating novel products or improving existing fasteners. Given the diverse probabilistic mechanical fasteners employed in nature, there is opportunity to further the research and development of these underdeveloped fasteners. To this end, we present a framework which describes the theory, design considerations, modelling, and mechanical testing required to study probabilistic mechanical fasteners. We further provide a comparison of the performance of existing probabilistic mechanical fasteners found in nature and industry as a reference for novel bio-inspired designs. Finally, we discuss current areas of application and future opportunities for fastener innovation. [DOI: 10.1115/1.4048448]

1 Introduction

The challenge of attachment has inspired a broad range of solutions in both industry and nature. Welding, gluing, and bolting technologies are some of the techniques devised in industry [1]. In nature, examples include mussels secreting sticky foot proteins in salt water [2], gecko footpads utilizing van der Waals forces [3], and some fruit hooks mechanically engaging with the fur or feathers of passing animals [4]. The underlying principles behind these attachment devices can be described as primarily relying upon chemical, physical, or mechanical joining. To date, most research and innovation efforts have been focused on exploring adhesive attachments utilizing suction [5] and chemical bonds [6–9]. Less attention has been devoted to purely mechanical attachments. Mechanical fastening is a practice that predates civilization, beginning with the invention of basic hooks, arrows, and barbed spears [1]. With the invention of hook-and-loop fasteners in 1955 [10], mechanical fastening technologies expanded to include an immense variety of attachment designs. Since the vast number of fastener elements results in a high likelihood of attachment, these devices are described as probabilistic mechanical fasteners.

Probabilistic mechanical fasteners are comprised of one or two specially designed surfaces with many hooking elements. Those with only one specially designed hooking surface interact with mating surfaces in their environment, which possess a degree of randomness, e.g., a surface covered in asperities of different shapes and sizes. The distribution of spacings between asperities has been found to follow an exponential distribution which drives the likelihood of a hooking element successfully engaging asperities on the mating surface [11]. For fasteners with two specially designed surfaces, such as a typical hook-and-loop fastener, the likelihood of attachment is certain given the high number of elements. Unlike other attachment technologies which involve additional tools and a high level of skill, these fasteners do not require expert precision to achieve secure attachments [12]. Other advantageous characteristics of these fasteners are that they are reversible, repeatable, and durable. These traits allow probabilistic mechanical fasteners to be employed in a multitude of applications including medicine, transportation and storage, apparel, and robotics.

Manuscript received April 6, 2020; final manuscript received September 5, 2020; published online October 7, 2020. Assoc. Editor: Dennis Kochmann.

The first artificial probabilistic mechanical fastener was inspired by nature. When the Swiss engineer de-Mestral was out hiking, he noticed tiny hooks of burdock seeds clinging to the fabric of his clothing. This discovery led to the creation of the first hook-and-loop fastener [13]. Since this discovery, there have been many variations of de-Mestral's original design. However, there have been only three bio-inspired designs based on probabilistic mechanical fasteners found in nature—one inspired by Galium aparine leaf hooks [14], the second by insect leg hooks [11,15,16], and the third by hooks surrounding the proboscis of gut parasites [17]. Given the wide popularity and use of these fasteners in industry, there is great potential to create novel products and improve existing designs by studying underutilized probabilistic fasteners found in nature. The focus of this paper is to present a framework to aid in the research and development of novel bio-inspired probabilistic mechanical fasteners.

In Sec. 2, a detailed description of a probabilistic mechanical fastener and the theory behind a successful attachment is described. Recently, the first directional probabilistic mechanical fastener was discovered between the overlapping flight feathers of birds. This discovery motivated our bio-inspired outlook for finding new functional fastener designs. Section 3 presents the design process for a bio-inspired mechanical fastener including fastener element design choices, material and manufacturing options, a modelling framework, mechanical testing, and an overall strength comparison with existing probabilistic fasteners found in nature and industry. In Sec. 4, we discuss current areas of applications and focus on opportunities in the field of robotics. We conclude Sec. 4 with a discussion of alternative design pathways to enhance a probabilistic mechanical fastener by harnessing innovative combinations of physical and bio-inspired principles.

2 Description and Theory of Probabilistic Mechanical Fasteners

Probabilistic fasteners are attachment devices comprised of many hooking elements forming an array. Each hooking element has a probability of attachment and combining many of the hooking elements into a single array provides a high likelihood of attachment [18]. To compare the functional principles of probabilistic fasteners with other biological attachments, we present an overview of the main fastening strategies found in nature as seen in Fig. 1. Successful attachment of probabilistic mechanical

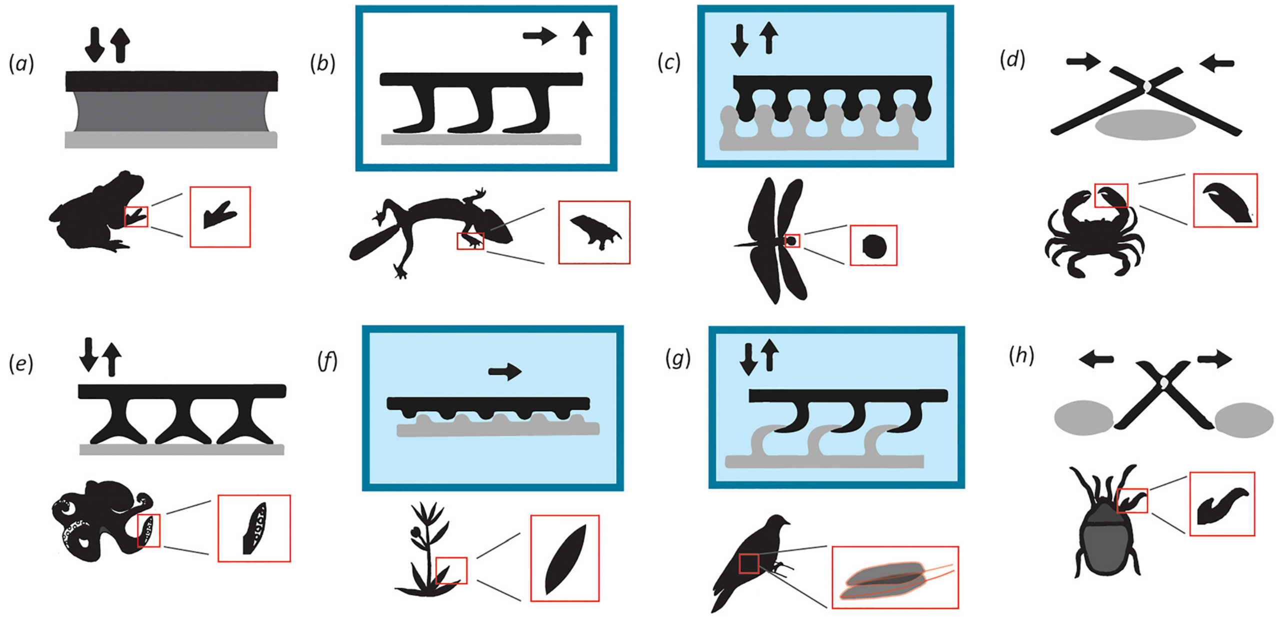

Fig. 1 Schematic function of eight attachment principles identified in nature [19], including: (*a*) Wet Adhesion in frog toe pads [20], (*b*) dry adhesion in gecko toe pads [3], (*c*) interlocking mechanism in the dragonfly head arrester system [21], (*d*) clamping of crab pincers [22], (*e*) suction in octopus tentacles [5,23], (*f*) friction for hooks on burr leaves [24], (*g*) hooking between overlapping microstructures in some bird species' flight feathers [25], and (*h*) spacing in the specialized setae on the shoulder joints of feather mites [24]. While many recent reviews on and innovations in bio-inspired attachment are based on the principles of adhesion and suction [5–9], less attention has been given to attachment devices that rely on passive mechanisms. To fill this gap, our review focuses on probabilistic mechanical fasteners, which are highlighted and outlined in blue. They are based on interlocking, friction, and hooking mechanisms. The unique characteristics of these micropatterned fasteners and their frequent appearance in nature provides unexplored opportunities for creating new bio-inspired fasteners. Drawings of attachment devices modified and reprinted with permission from the *Royal Society* [19,24]. Animal and plant avatars were hand drawn.

fasteners does not require engagement of each individual hooking element, but rather a "sufficient number of contacts" [18,19]. When the hooking elements are brought into contact with a mating surface, the engagement of elements is primarily passive due to the high likelihood of attachment. The bond between the hooking elements and mating surface is unique in that it can be broken and rejoined many times. This is due to the many elements in the array; while some of the connections may destructively fail under loading, there are enough elements to ensure that a "sufficient number" is still functioning for successful reattachment [18,19]. All that is required for joining is to actively bring the fastener elements into contact. As a result, attachment is highly likely based on each element of the array having a high likelihood of attachment. Although the miniscule scale of each hooking element produces only a small contact force, the integrated result of many hooked elements is a secure connection. Together, the hooking elements contribute to make a strong, reversible, and repeatable attachment which requires little precision in aligning the hooking elements with the mating surface.

2.1 Mating Surfaces for Probabilistic Mechanical Fasteners. The mating surface can have purposefully designed, patterned elements or a degree of randomness in its elements' geometries. A description of the differences between these mating surfaces is shown in Fig. 2. A predetermined, patterned mating surface can have hooking elements identical to the fastening surface, as in self-mating, or it can involve different element geometries meant to engage a hooking surface, such as loops. Probabilistic fasteners in nature most often engage with random mating surfaces encountered in their environment [17–19]. In manufacturing, predetermined, patterned mating surfaces are specifically designed and sold together with the fastener surface, as in hook-and-loop type fasteners. For patterned surfaces, where each mating element is designed to engage, the likelihood of attachment is essentially guaranteed [17–19]. In contrast, a mating surface with a degree of randomness cannot guarantee a successful attachment. Differences between the likelihood of attachment for patterned and random mating surfaces is illustrated in Fig. 3. Besides the random quality of the mating surface, there are additional factors which impact the likelihood of attachment including: hooking and mating element spatial distributions, variable element strengths, and the angle of the applied load. Therefore, it is worth examining the factors which influence a successful attachment for the purpose of designing probabilistic mechanical fasteners.

2.2 Theory Behind the Likelihood of Attachment

2.2.1 Background for Examining Failure in a Matrix of Many Elements. Probabilistic mechanical fasteners consist of many elements which effectively form a single matrix. The first attempts to explain the performance of a matrix with many individual elements examined composites made of fiber bundles [28,29]. Failure of the matrix resulted from failure of individual fibers due to crack formations. Strain mismatches between the individual fibers led to reduced crack strength. Strain mismatches also made fibers more susceptible to slip [28,29]. Later, the stress needed to overcome bonding at the fiber-matrix interface was also determined to influence the overall matrix cracking stress [28,29].

For a matrix of many individual fiber elements, the evolution of fiber failure which leads to overall matrix cracking, has been examined through the concept of load sharing [30,31]. Load sharing is the mechanism through which matrix elements redistribute and share load when a single element fails. Load sharing can be viewed from two perspectives: global load sharing, and local load sharing. Global load sharing assumes that broken fibers do not cause local stress concentrations, and that load lost by failed fibers, n, is transferred equally to all unbroken fibers, $n_f - n$. The

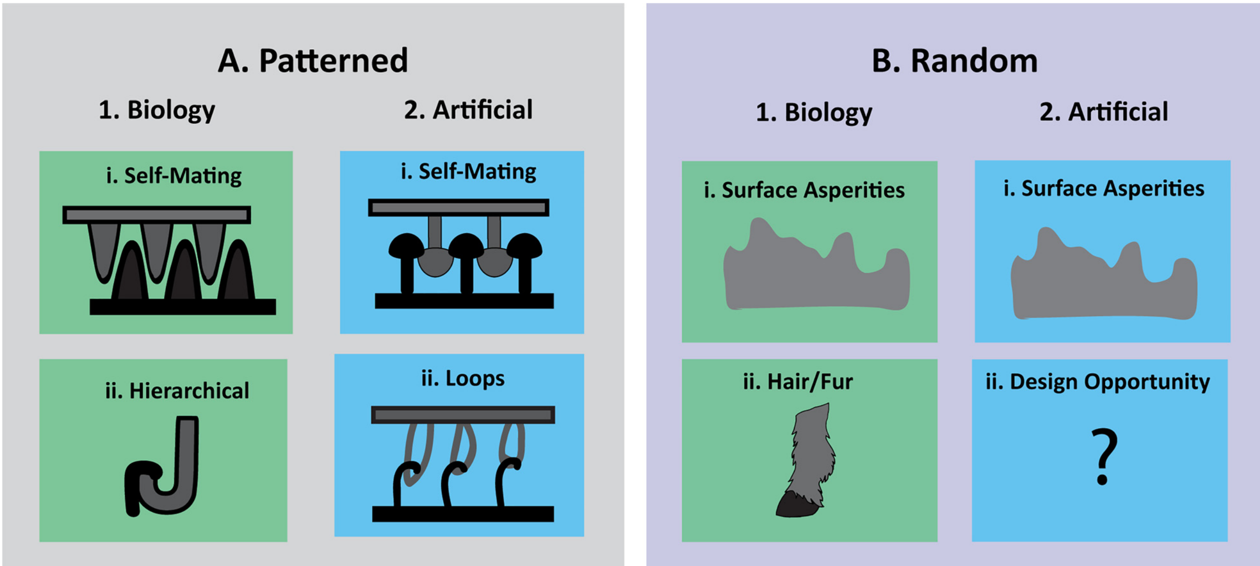

Fig. 2 Patterned (*a*) and random (*b*) mating surfaces of probabilistic mechanical fasteners. Patterned mating surfaces, (*a*), are predetermined to engage with the fastener surface featuring hooking elements in a specific fashion. Random mating surfaces, (*b*), are adapted to engage with hooking fastener surfaces encountered by chance in the environment. In nature, a patterned mating surface can be self-mating, (a(1.i)), or hierarchical, (a(1.ii)). A self-mating surface is identical to the hooking element surface. An example of a self-mating surface in biology is the head-arrester system in dragonflies (Fig. 1(*c*); [21]). A hierarchical connection involves hooking and mating elements of different scales. Hierarchical connections can be found in wing interlocking devices of insects [19], well-described fastening structures between the barbs of a single feather vane [26], and between the recently discovered directional fastening microstructures of overlapping flight feathers (Fig. 1(*g*); [25]). Random mating surfaces in biology include surface asperities, (*b*(1.i)), as well as feather and furry surfaces, (*b*(1.ii)), which engage with the hooks of insects and plants. Most artificial mating surfaces are patterned and are made of self-mating or loop elements although some artificial hooking element surfaces have been designed to engage with surface asperities (*b*(2.i)), [11,15,16]. To our knowledge there is currently no artificial equivalent of hair, fur, or feather structures for probabilistic mechanical fasteners. Drawings modified from [15,19] and printed with permission from *Sage Publication Inc. Journals* [15] and the *Royal Society* [19]. Image of animal hair is hand drawn.

increase in load for the unbroken fibers is given by the expression $[\frac{1}{n_f-n}]\Sigma_{i=1}^{n}\Delta\sigma_i(z)$, where $\Delta\sigma_i(z)$ is the change in stress that results at a position z along the length of the nonfailed fibers [31]. As all unbroken fibers experience an equal increase in stress, it is further assumed that both the stress at each fiber is the same and the strength distribution along the lengths of all fibers is the same [31]. This assumption is shown in Eq. (1) which can be used to find the resulting stress due to the applied external load and the redistributed stress that results from load sharing. In Eq. (1), the resulting stress is T, the applied external load is σ_f, and the redistributed stress from load sharing is $\Delta\sigma_i(z)$. The redistributed stress, $\Delta\sigma_i(z)$, depends on the height, z, along the length of a fiber, while the external load, σ_f, is independent of the height along the fiber [31]. Because the stress on each fiber and the strength distribution along the length, z, of each fiber is assumed to be the same, the resulting stress, T, can be assumed to be the same across the length of the fibers [31]. As a first approximation, Eq. (1) can be used to calculate the resulting stress on a matrix of fibers, or fastener elements, due to an applied external load and stress redistribution resulting from load sharing:

$$T = T(z) = \sigma_f + \frac{\mathrm{n}}{n_f - n}\left[\frac{1}{n}\Sigma_{i=1}^{n}\Delta\sigma_i(z)\right] \tag{1}$$

With the simplified assumptions of global load sharing, criteria for measuring the performance of a matrix can be developed for expressions of fiber pull out lengths, work of pull out, and ultimate tensile stress [30]. In contrast to global load sharing, local load sharing considers local stress concentrations, stress gradients, and localized damage due to notches, holes, or other imperfections [31]. When a fiber is damaged, the stress increases in the region of the failed fiber which propagates damage from one region to another nearby region [31]. There are several models which have been developed to characterize local load sharing, see Curtin [31] and additional references for further explanation of load sharing [31–36].

2.2.2 Likelihood of Attachment for Case of Probabilistic Mechanical Fasteners. For probabilistic fasteners, the criteria for success and failure depends not only on the fracture and load sharing of hooking elements, but also on the likelihood of attachment with a mating surface. Here, we discuss the likelihood of attachment between a spine hooking element and a random asperity mating surface [11,15,16,37]. We present the primary factors that impact successful attachments as a basis for examining the likelihood of attachment for different fastener and mating surfaces. The loading and release of a hooking element with an asperity is described as a loading cycle and consists of four main phases (Fig. 4): approach, surface contact, asperity encounter, and release. Each phase has key factors that impact the likelihood of a successful attachment [11]. These attachment factors are discussed first from the perspective of compliantly supported, rigid spines [11]. Later, we examine how the phases of attachment differ for compliant hooks.

During the approach phase, the hook moves with a horizontal and vertical velocity until it contacts the asperity surface [11]. Here, the approach angle primarily determines the hook's ability to engage with an asperity [11]. If the hook's approach angle is too high, the hook may bend when it reaches the asperity surface. On the other hand, if the hook's approach angle is too low, the hook may slip when it contacts the asperity surface [11]. During the surface contact phase, the spine slides along the surface to find a viable asperity and applies a small positive normal force and may also apply a small shear force to the surface [11]. Factors that determine the probability of latching onto an asperity are loading force, load angle, and the coefficient of friction of the surface

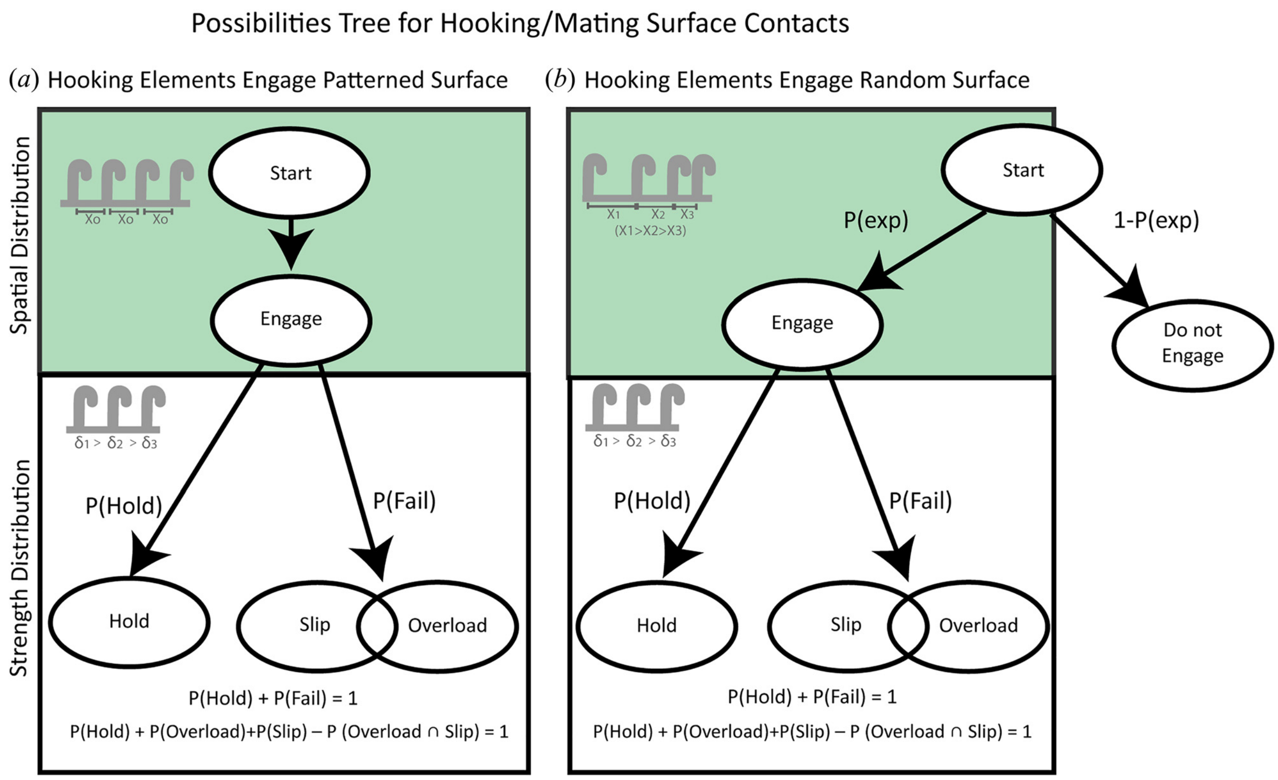

Fig. 3 Likelihood of attachment between a hooking surface and its patterned/random mating surface. Successful attachment of a hooking element depends on the spatial distribution of mating elements and on the strength of the connection of each engaged element. For a patterned mating surface, engagement is guaranteed since the spatial and strength distributions are optimized to engage by design. On the other hand, a mating surface with a random spatial and strength distribution is not guaranteed to engage. Statistical models have been developed to explain the likelihood of attachment for claws [27] and spines [15] interacting with rough asperity surfaces. Once the hooking and mating surfaces engage, there are two possibilities for the contact: it can hold or it can fail. These outcomes are described by the expression, $P(\text{Hold}) + P(\text{Fail}) = 1$, which is adapted from Ref. [15]. Failure occurs through overload, slip, or simultaneously from both overload and slip. We then assume that $P(\text{Slip})$ and $P(\text{Overload})$ are independent, nonmutually exclusive events as shown above in the Venn Diagrams for Slip and Overload. From these assumptions, we represent $P(\text{Fail})$ as $P(\text{Fail}) = P(\text{Overload}) + P(\text{Slip}) - P(\text{Overload} \cap \text{Slip})$. Substituting this expression into $P(\text{Hold}) + P(\text{Fail}) = 1$, and rearranging gives $P(\text{Overload}) + P(\text{Slip}) - P(\text{Overload} \cap \text{Slip}) = 1 - P(\text{Hold})$. The likelihood of each scenario may evolve if the conditions of the attachment are dynamic. For example, if the loading force causes failure of hooking elements, load sharing will require nonfailed elements to sustain more force which would increase $P(\text{Overload})$. On the other hand, if the connection was displaced so that the hooking element lost its ideal grip on the mating surface, $P(\text{Slip})$ would increase. For both an increase in load and displacement of the hooking element, $P(\text{Overload})$ and $P(\text{Slip})$ would increase. Diagram modified and printed with permission from *Sage Publications Inc. Journals* [15].

[11]. The coefficient of friction of the surface is important, because it determines whether the hook may fail in strength (rough surface) or from slip (smooth surface) [11].

In the asperity encounter phase, the motion of the hook is halted by an asperity [11]. The normal force component due to surface friction pulls the hook towards the mating surface, which opposes the loading force [11]. Contact with an asperity depends on the spatial distribution, slopes, and shapes of the asperities, as well as the relative size of the spine tip radius compared to the average asperity size [11,16]. The spatial distribution of lengths between asperities on a mating surface were first described using an exponential distribution [11]. In Table 1, variations of this general expression are presented for specific cases [15,16]. In addition to asperity spatial distribution, asperity slopes also influence whether or not a hooking element can engage the mating surface [11]. An expression for the minimum usable asperity slope is found in Table 1 [11].

As the hooking element approaches an asperity, it is critical to consider the size of the hooking element's tip radius—if it is too large, the force of attachment increases, but it misses the chance to engage smaller surface asperities [11]. One solution is to use a higher number of smaller hooks to achieve the same integrated force of attachment and reach the smaller asperities. At some point, however, load sharing is impeded as too many hooking elements will interfere with each other's attachments, blocking some hooking elements from carrying the load [11]. With this unequal distribution of the load, the force ceases to increase with the number of hooks. Relationships between hooking element size and the number of hooking elements is found in Table 2.

From the specific perspective of spine and asperity contacts, release of a connection can result in two ways: (1) the loading force can overload the attachment force and break the connection, or (2) the hook can be pulled at an angle which stretches the hook until its tip slips off the asperity [11]. While these factors were developed based on the study of compliantly supported, rigid spines [11], the principles can be applied to compliant elements with more considerations.

As many hooking elements in biology often have more compliant behaviors then those used in engineering technologies [4,22,24–26,29], we discuss some of the considerations and differences for compliant versus rigid hook behavior during the approach, surface contact, encounter, and release phases of attachment. Compliant structures undergo greater deflections then rigid structures from an identical external load [39,40] as their flexible structures are more capable at absorbing and storing energy [41,42]. Furthermore, compliant hooks have been found to experience higher deflection under dynamic loading then under static force [40]. According to the magnitude and static/dynamic

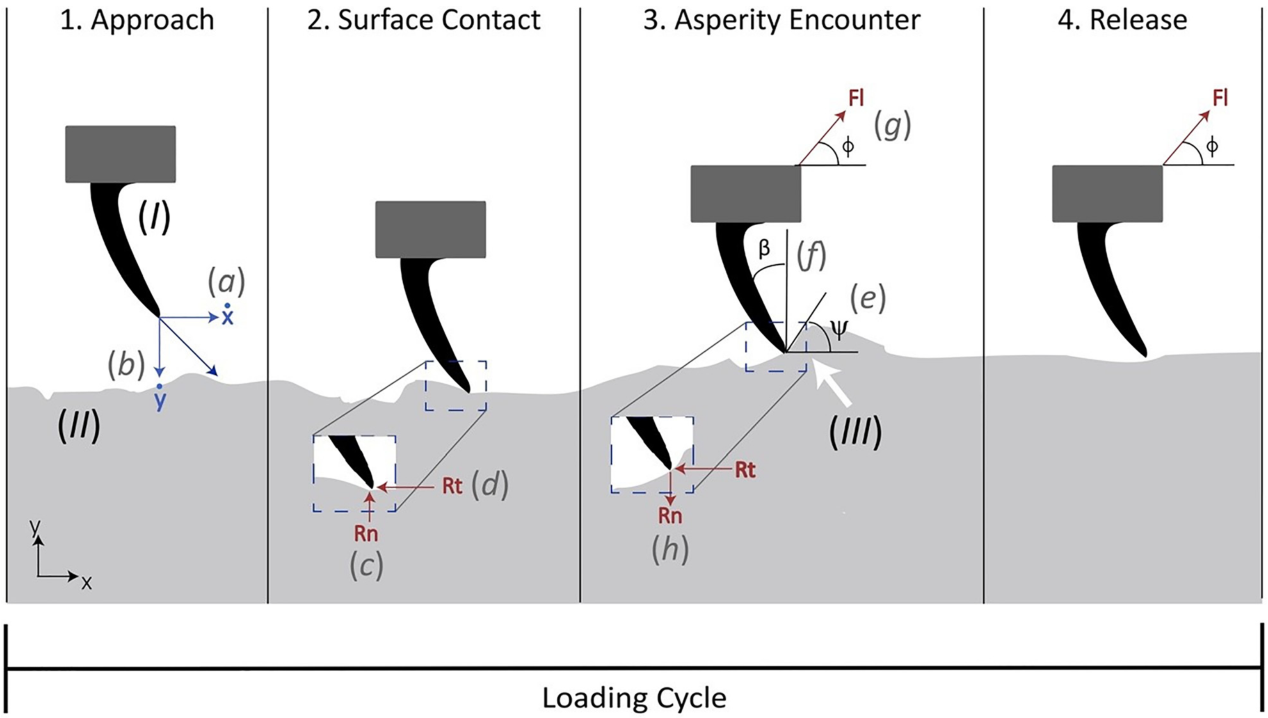

Fig. 4 The loading cycle of a hooking element with a random asperity mating surface. The loading cycle includes four phases: 1—Approach, 2—Surface contact, 3—asperity encounter, and 4—release [38]. After moving with a horizontal (*a*) and vertical velocity (*b*), the hooking element (I) contacts with the mating surface (II), which exerts a small normal (*c*) and shear (*d*) force at the tip of the hooking element. The hooking element is then dragged until it encounters an asperity (III) at which point the angled (ϕ) loading force (*g*) tries to pull the hook away from the mating surface in the vertical (y) direction. The vertical pull force is opposed by the normal component of the tangential surface friction force (h), which pulls the hooking element towards the mating surface. In (III), the local surface slope of the asperity (Ψ) combined with the angle of the tip of the hooking element (β) is also shown to be key for fastening function. Eventually the loading force overcomes the normal component of the friction force and the hook is released. Schematic modified and printed with permission from *Sage Publications Inc. Journals* [15].

Table 1 Expressions for asperity distributions and usable asperities

Asperity distribution	PDF expression	Variables
Asperity spatial distribution [11]	$f(x;\lambda) = \lambda exp(-\lambda x), x \geq 0$ (2)	λ: number of asperities x: random variable for distance between asperities
Asperity spatial distribution considering asperity length [15]	$P(\alpha,\lambda;x) = \alpha P_{\text{exp}} + (1-\alpha)P_{\text{int}}$ (3)	P_{exp}: spacing between asperities P_{int}: asperity length $(1-\alpha)$: probability of immediate engagement α: fit parameter λ: number of asperities x: random variable for distance between asperities
Asperity spatial distribution for linearly constrained hook [16]	$f_\psi(\psi) = \frac{2}{\delta\psi} = \frac{2}{\delta\psi^2}(\psi - \psi_{\text{min}})$ (4)	ψ: asperity slope. When $\psi > 60$, distribution is linear and not exponential
Usable asperity slopes [11]	$\theta_{\text{min}} = \theta_{\text{load}} + arccot(\mu)$ (5)	θ_{min}: minimum usable asperity slope θ_{load}: angle of the applied load μ: coefficient of friction

Note: This table includes equations which can be used to determine characteristics of a random asperity mating surface. Here, we reference three equations which explain the spatial distribution of asperities, including a general asperity distribution in Eq. (2), a spatial distribution which takes into account the length of the asperities in Eq. (3), and an asperity spatial distribution for the special case of linearly constrained hooks in Eq. (4). These equations are presented as a starting point for readers seeking to research or design fasters which interact with random asperity surfaces. Understanding different expressions for asperity spatial distributions can aid in creating hooking surfaces which are more likely to contact the asperity mating surface. Additionally, we reference an expression for determining which asperities on a random mating surface can sustain a connection with a hooking element based on the asperity's slope.

Table 2 Expressions for stress, strength, and load sharing in hooking elements

Load on hooking element	Scaling relation	Variables
Force carried by one hooking element [37]	$F_1 = F_h \propto \frac{r^4}{R^2}$ (6)	F_1: force for one hooking element F_h: max attachment force, see (8) r: radius of an equivalent circular cross section R: hook radius of curvature
Force scaling for multiple hook subcontacts [37]	$F_n = n^\beta F_1$ (7)	n: number of subcontacts F_1: force carried by one hook F_n: force for n subcontacts $\beta = 0$ if $r \propto R$ $\beta = 2$ if $r = \text{constant}$
Bending [37]	$\sigma_b \propto \frac{r}{R}$ (8)	σ_b: bending stress r: radius of an equivalent circular cross section R: hook radius of curvature
Tension [37]	$\sigma_t \propto \left(\frac{r}{R}\right)^2$ (9)	σ_t: tensile stress r: radius of an equivalent circular cross section R: hook radius of curvature
Nominal Stress [37]	$\sigma_h \propto \frac{r}{R}$ (10)	σ_h: nominal stress r: radius of an equivalent circular cross section R: hook radius of curvature
Hook/asperity contact strength [11]	$F_{\text{hook/asperity}} \propto r^2$ (11)	r: radius at tip of hooking element $F_{\text{hook/asperity}}$: load per hook/asperity contact

Note: While load sharing can involve intense modelling and mathematics [31–36], there are also simple expressions which can intuitively guide the examination of stress and strength in fastener elements. Equations (6) and (8)–(11) describe how fastener element strength and stress are influenced by the radius of the hooking element. Equation (7) relates how force carried by multiple hooking elements compares to the force carried by a single hooking element.

behavior of the loading force, the geometry of the compliant hook will deflect and adapt as it approaches the mating surface.

Once the compliant hook meets the mating surface, its structure will displace under loads from the external force and mating surface. As a result, the compliant hook experiences reduced friction on the mating surface, and therefore less wear, compared to rigid hooks [41]. The deflections of the compliant hook can be highly complex, and the underlying material properties may not be known [41]. One way to better understand the material properties, and therefore behavior of a compliant hook, is to determine the Young's modulus by creating Force versus Displacement curves [39,40] or performing a cantilever test [24]. Further analysis of compliant hook behavior can be undertaken through modelling [41–44].

A challenge that compliant hooks are more likely to experience than rigid hooks upon encountering an asperity or other mating element is the collision of multiple compliant hooks [41]. This collision prevents an attachment from being made with the mating surface. Collision of compliant hooks is due to their highly deflective structures which can interfere with the performance of the fastener. When designing compliant fasteners, care should be taken to consider the spacing between the hooking elements. Finally, at the release of an attachment, compliant hooks do not exhibit the backlash seen in rigid structures [41]. Being aware of the factors which influence a secure connection for an attachment with random mating surfaces can aid in designing fasteners which are more likely to attach.

2.3 Focus on Biological Probabilistic Mechanical Fasteners. Probabilistic fasteners evolved in nature under natural selection of the species featuring them. For example, parasitic worms have large numbers of hooks to ensure attachment to a host organism [17,22]. Eggs of some fish have hooks which keep the eggs joined in strong river currents, and insects such as fleas, bat flies, and beaver beetles have tiny hooks which entangle in the fur of host animals [22]. Along with hooks of fruits [4,29], some plants have hooks on their leaves which aid in attachment and orientation towards sunlight [14,24]. Certain flowers and leaves also have surfaces that promote attachment with hooks on insect feet to aid pollination [45,46]. Most of the probabilistic fasteners in nature have one specialized fastener surface which evolved to interact during chance encounters with a wide range of surfaces in the environment (see Fig. 2 for a reference of the different types of mating surfaces). However, there are several examples of probabilistic fasteners in nature with a patterned, predetermined surface such as wing interlocking devices of beetles [47–50], head arresters in dragonflies [18,21] (see Fig. 1), and bird flight feathers. A bird feather is made of a central shaft called a rachis, from which angled projections called barbs branch [22,25,26]. Branching from the barbs are even smaller angled projections called barbules. Barbules from adjacent barbs interlock via small hooks, or hooklets [22,25,26]. Together, the many hooked barbules zip up the feather to form a uniform surface [22,25,26]. The interactions between microstructures of a single feather hooking to form a uniform surface has been studied since the 1930s [51] and is now well understood [52–54].

Recently, a new class of probabilistic mechanical fasteners has been discovered between overlapping flight feathers in many species of birds (apart from silent fliers such as owls) [25]. Whereas the function and performance of the hooklet-based fastening mechanism between the barbs in a single feather vane are generally known and understood [25,54–58], there also exists a fastening mechanism between overlapping flight feathers, as seen in Fig. 5 [25]. Engagement of this feather-feather fastener takes place between hooked structures protruding down from the overlapping feather surface and protruding up from the underlying feather surface [25], see Fig. 5. This fastener is uniquely directional—only when the feathers are pulled away in tension, as when a bird extends its wings, do the microstructures engage to

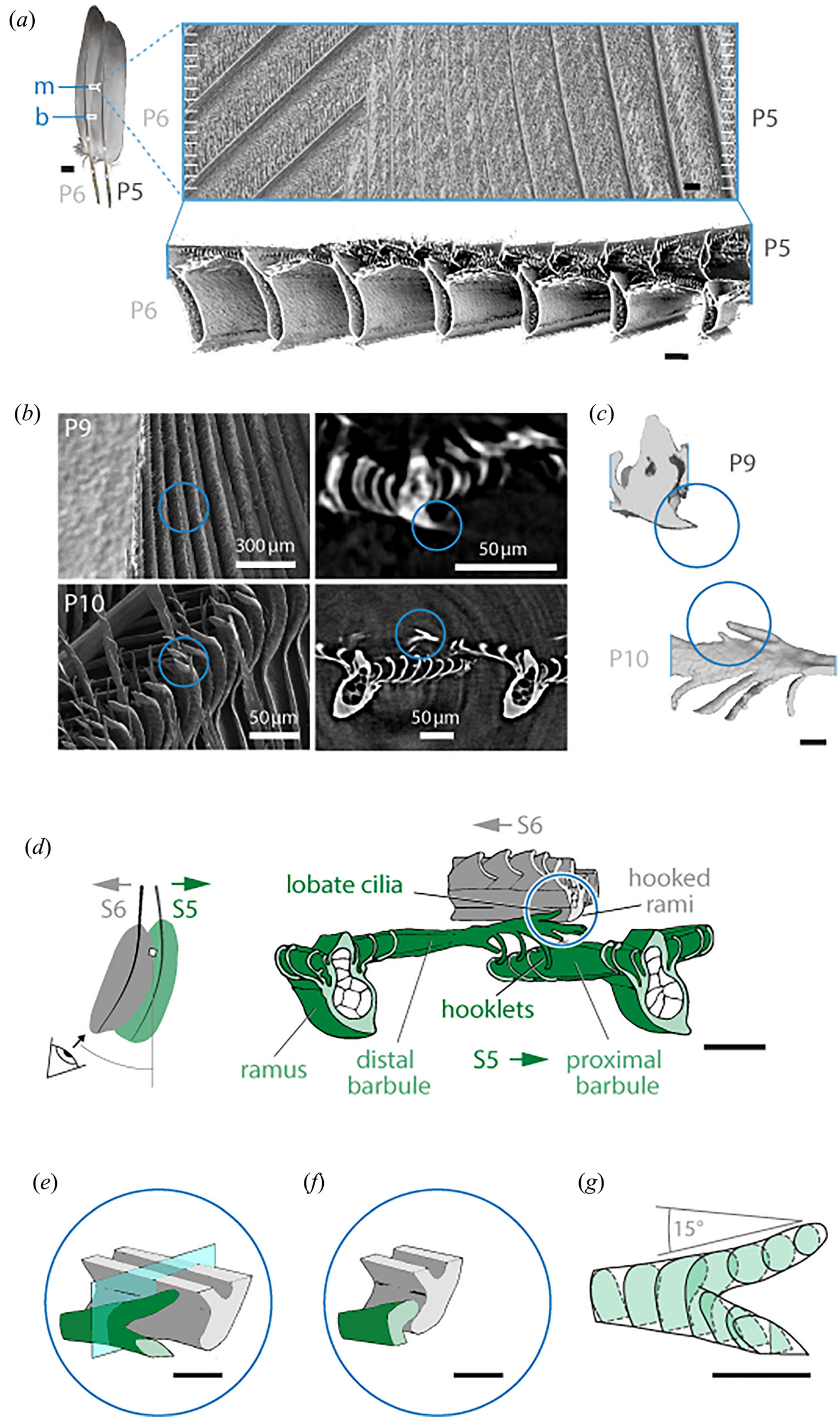

Fig. 5 Unique directional mechanical probabilistic fastener between bird flight feathers based on two differently patterned mating surfaces [25]. (*a*) X-ray microscope micro-CT reconstruction of the directional micromechanical fastening mechanism between primary flight feathers P6 and P5 of a rock pigeon (Columbia livia). These microstructures are directional and engage when loaded under tension as when the bird extends its wings. This mechanism has been found between the primary, secondary and tail flight feathers of a large number of bird species except silent fliers such as barn owls (Tyto alba) [25]. The scale bar for the macroscopic view of P5 and P6 feathers is 1 cm. The scale bar for the microstructure CT view is 100 μm. (*b*) SEM images of

the mating surfaces of the overlapping (P9) and underlapping (P10) side of two primary feathers that can fasten directionally in a pigeon wing. P10 images reveal the hooked rami ridges which interact with a field of lobate cilia that stick up and out of the underlying P9 feather's dorsal plane. This fastener is hierarchical, meaning that the interacting fastener elements are different scales: the hooked rami sit at the underside of barbs, whereas the hooked lobate cilia stick out on the upper side of specialized fastening barbules. (*c*) Beamline nano-CT reconstruction of the hooked quasi-2D rami and hooked 3D lobate cilia. The downward hooked rami tip is circled and so is the lobate cilia extending up and out of the dorsal feather surface. Note these cross section do not show the actual hooking engagement orientation. The scale bar is 10 μm. (*d*) 3D reconstruction of the in vivo fastening between two secondary flight feathers (S5, S6) drawn to scale based on nano-CT scans. The reconstruction shows the classical interbarb fastener that connects the distal and proximal barbule via hooklets and sticks all the barbs together in a feather vane. Remarkably, the same distal barbule featuring the hooklets can also feature the 3D hooked locate cilia that fastens the hooked rami of an overlapping feather directionally. The two fasteners are oriented approximately perpendicular, decoupling their functions. The interfeather fastener is only found between the trailing vane of the overlapping and the leading vane of the overlapping flight feathers. (e, f, g) Zoomed in (cross-sectional) nano-CT reconstruction of the directional fastening mechanism between a single hooked rami and lobate cilium. The slanted tip of the lobate cilium helps ensure the two feather surfaces mate. Scale bar 10 μm. Images adapted from Ref. [25].

impede feather separation and ensure a continuous aerodynamic surface without gaps. As this fastener engagement is dependent upon direction, we term this mechanism a directional probabilistic fastener [25]. Directionality between significantly fewer hooking elements connecting front and hind wings is also observed during wing extension in some insects [47–50]. The directional mechanical fasteners described here, are analogues to anisotropic adhesion observed in setae (small hair projections on gecko feet [3]). Depending on the angle of pull, the setae's adhesion strength is either maximized or dramatically decreased [59]. This ease of switching between strong and weak adhesion can be ideal for creating a robust, releasable adhesion [59].

What sets the feather-feather directional probabilistic fastener apart from insect wing locking and even gecko setae, is not only the orders of magnitude higher number of hooking elements, but also the hierarchical engagement of microstructures [25]. The trailing vanes (vanes projecting from one half of the rachis which encounter aerodynamic forces after the leading edge vanes [22,25,26]) of flight feathers are comprised of specialized fastening barbules that feature lobate cilia (3D hook shaped protrusions on the upper surface of the barbule that stick up and out of trailing vane surface [25]). These lobate cilia latch stochastically onto rami (quasi 2D hooks pointing down from the barbs of the overlapping feather's leading vane). See Figure 5 for a visual of engagement between lobate cilia and rami. While both the hooked rami (hierarchical level of the barb) and lobate cilia (hierarchical level of the barbule) are of the order of ten micrometers, the hooked rami are many millimeters to centimeters long; however, the number of lobate cilia (1000 s) is much higher than the number of hooked rami (10–100 s) and a sufficient number of lobate cilia is able to secure the rami hooks under tension [25]. The structure of the feather vane cross section ensures that the underlapping and overlapping feather surfaces are correctly aligned and in contact to securely fasten [25]. According to our literature review, there is no equivalent biological or technological fastener. Given the diversity of probabilistic mechanical fasteners found in nature, many with traits that have yet to be characterized or translated into artificial fasteners, there are numerous opportunities to research and develop innovative bio-inspired mechanical fasteners.

3 Design Framework for Bio-inspired Fasteners

In this section, we discuss a design framework for developing novel bio-inspired fasteners that can be applied generally, including for our specific focus on probabilistic mechanical fasteners. The design framework, Fig. 6, has been distilled and developed based on established general design diagrams as well as bio-inspired design diagrams found across literature [27,60–62]. Fastener innovation generally arises from observations, such as noticing a shortcoming in current fasteners or discovering a problem that a novel fastener could solve. For bio-inspired fasteners, it is the observation of a biological mechanism that leads to new designs (e.g., the original observation of de-Mestral resulting in hook-and-loop fasteners). Bio-inspired design builds off characterizing the biological fastener's function. Performing imaging techniques [14,18,19,24,39,63,64], and mechanical testing [14,18,23,39,40] (as well as other physical characterization processes) reveal the biological fastener's underlying structure and attachment principle(s). This leads to a general understanding of the biological fastener's method of attachment. Key behaviors and traits of the biological fastener can then be understood and inform engineering design choices such as the fastener elements' geometries, material properties, and method of manufacturing [14,17]. Once a design of the bio-inspired fastener has been determined, it can be evaluated using modelling, simulations, and mechanical performance tests. Comparison between the biological fastener and bio-inspired fastener based on metrics, such as max force per hooking element, can further aid in design evaluation and optimization. Iteration of this design framework can improve the bio-inspired fastener design and lead to new understandings of probabilistic mechanical fasteners.

3.1 Designing Fastener Element Structure.

Probabilistic mechanical fasteners are made up of many individual hooking elements whose purpose is to catch and secure element(s) on the mating surface. The basic structure of a hooking element includes a base, stem, and grip as seen in Fig. 7 panel (*a*). The base grounds the hook into the fastener substrate while the stem determines how the hook protrudes from the substrate surface. The grip engages the mating element(s). Different geometries of hooking elements have been proposed to improve the hook's ability to catch and secure the mating surface [72,75–94]. Some examples are shown in Fig. 7 panel (*b*).

Most variation in hooking element geometry involves the grip. There are three broad categories of fastening elements based on commonly used grips, as shown in Fig. 7 panel (a). The first category includes J-shaped grips, also known as crook grips due to a resemblance to a shepherd's crook. [13,68,74–79,86, 95–99]. Second, so-called mushroom, or capped grips, which can be imagined as a crook grip rotated in space [67,99–110]. Third, Stem based grips which lack the curvature found in crook grips [110,111]. Finally, another category could be considered to include ridges, which are formed by projecting a hook in space [71,112]. Complexity in grip design can further be introduced by varying the number and geometries of grips on a single element. A single fastener surface can also include hooks with variable geometries

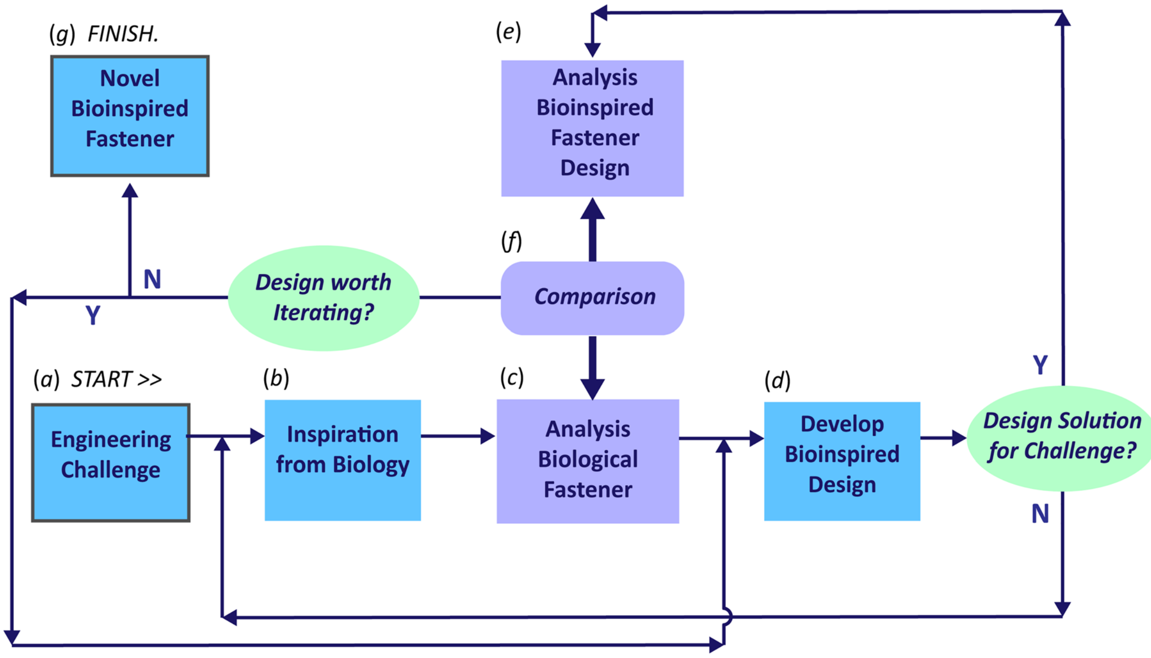

Fig. 6 Bio-inspired design process for inventing new high-performance mechanical fasteners. Through a review of proposed design methods [60], and bio-inspired design methods [27,61,62], we have developed a design approach for bio-inspired mechanical fasteners. (*a*) The approach begins with identifying an Engineering Challenge, which cannot be solved satisfactory with existing fasteners. (*b*) New design solutions can be engineered by drawing Inspiration from Biology. An organism suitable for the fastening challenge can be identified through a search of the literature and collaborating with a biologist who is an expert on the functional morphology of the organism of interest. (*c*) Once an appropriate organism is selected, the underlying physical principals is investigated by performing a rigorous scientific Analysis of the Biological Fastener. Analysis of the fastener often involves characterization through imaging techniques and mechanical testing as well as other physical characterization methods. (*d*) With characterization of the biological fastener complete, the next step is to develop the bioinspired design by translating the biological fastener's biological and physical principles into engineering analogs. Considerations for selecting engineering analogs involve determining fastener element structure and selecting a material and method of manufacturing. (*e*) An analysis of the bio-inspired fastener is then performed through mechanical testing, modelling, and simulations. Ideally, the analysis methods for the bio-inspired fastener are sufficiently similar to those of the biological fastener so that a reasonable one-to-one comparison can be made to evaluate the performance of the engineering design. The purpose of the comparison is to determine if the bio-inspired design sufficiently captures the desired performance features of the biological fastener. If the bio-inspired design captures the desired traits of the biological fastener, it can be iterated through by returning to (*d*) and further develop the bio-inspired design. On the other hand, if the comparison (*f*) reveals that the bio-inspired design fails to capture the desired mechanical fastener traits needed, a new organism and associated biological fastener can be selected by returning to getting inspiration from biology (*b*). The bio-inspired design is iterated until it is determined that it provides a sufficiently meets the requirements to solve the engineering challenge at which point a novel bio-inspired fastener (*g*) has been developed.

[113], spacings [71], and orientations [93], see Fig. 7 panels (*b*) and (*d*).

Given the vast multitude of variations that are possible for hooking element geometry, we have identified a simplified list of parameters, see Fig. 7 panel (*c*), to aid in the discussion and design of hooking elements. These ten design parameters are based on geometric parameters discussed across the literature [4,18,39,72,78,79,82,86,95,96,114,115] and include: total height, width of the base, width of stem at the "neck" transition to the grip, angle of the stem with respect to the base, angle of the neck with respect to the base, and grip height, width, length, span, and angle of curvature. Understanding relationships between these parameters is also valuable in designing hooking elements. Ratios between geometric parameters of fruit hooks have been found to greatly influence separation force [4]. Before settling on a hooking element geometry however, one must first consider the mating surface with which it will engage.

The structure of the mating surface is the primary constraint on the design of the hooking elements as it limits hooking element design. In the case of a loop mating surface, the hooking elements are constrained by how far the loops protrude from the mating surface substrate, as well as by the strength, number, and organization of the loops. Loop surfaces are often knitted [116–118], woven [69,119–122], or laminate [123–127]. While there has been progress improving the loop design to engage with hooking elements [67,72,113,117,125,129,131–141], there has been greater focus on improving hook designs to secure loop elements. For example, increasing the number of grips to catch more loops [70,79,82,84,85,87,94,114,141–143] adding variable heights to hooking elements to secure longer and shorter loops [69,141,144], and even combining hooks and loops onto a single fastener surface [145], are some of the strategies devised to enhance a hooking surface's ability to catch and secure connections on the loop surface.

3.2 Choosing a Material and Method of Manufacturing. When selecting materials and methods of manufacturing, it is important to consider the purpose of the probabilistic mechanical fastener. Since these fasteners are required to maintain a secure contact after repeated use, materials that offer both sustained strength and flexibility are ideal. Common manufacturing and material combinations for probabilistic mechanical fasteners are shown in Table 3. The early probabilistic fasteners were woven

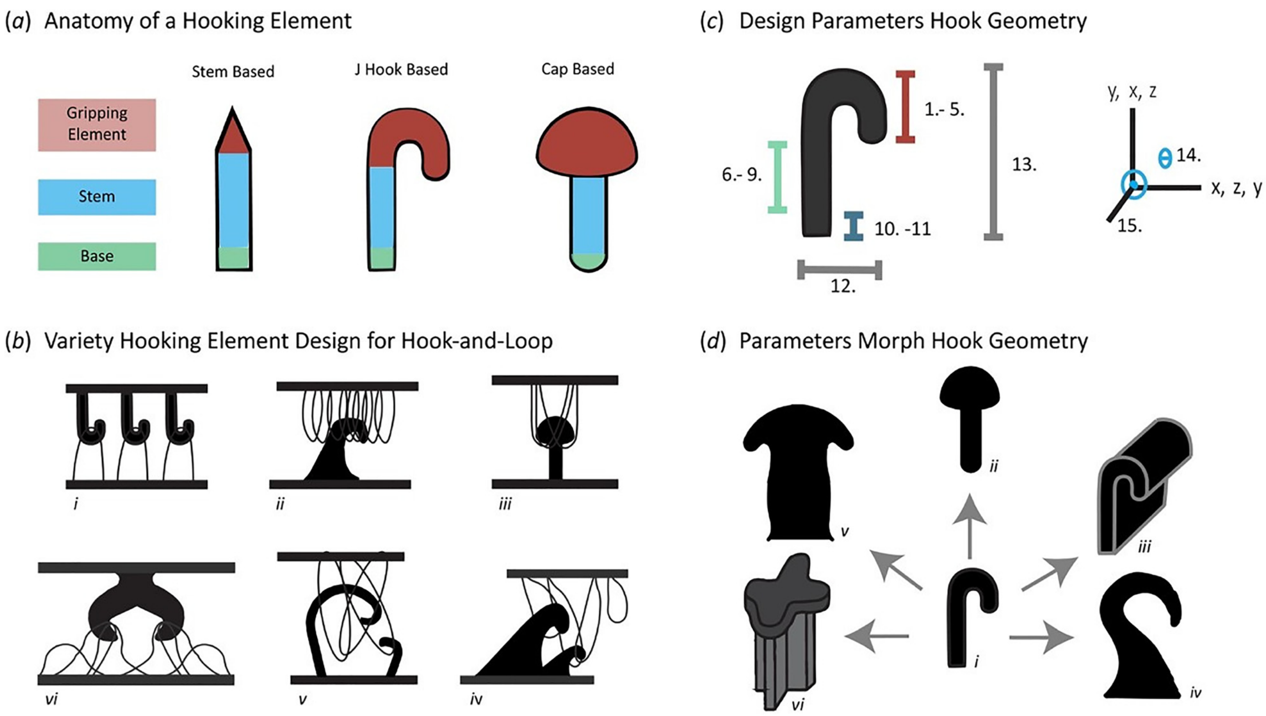

Fig. 7 The anatomy and geometric parameters of a fastener's hooking element. (*a*) Anatomy of a hooking element described in terms of a base, stem, and gripping element. The three basic hooking element shapes are stem- based [65], J-shaped [66], and capped [67]. The base secures the hooking element into the substrate, the stem determines how the hooking element rises from the substrate surface, and the gripping element is the primary component to interact with the mating elements. (*b*) Diversity of existing hooking element designs for hook-and-loop fasteners. Numerous designs have been claimed in patents to improve catching and holding loop elements. J-shaped hooks engage with one loop [65], (i); one J-shaped hook engages with multiple loops [64], (ii); a capped mushroom hook engages with multiple loops [68], (iii); different sized J-shaped hooks in parallel engage loops at different lengths [68], (iv); different sized J-shaped hooks in opposition engage loops at different lengths [69], (v); hook with two gripping elements engages with multiple loops [70], (vi); (*c*) General design parameters for hooking element geometry. The grip can be described by five parameters: width (1), length (2), span (3), angle of curvature (4), and number of gripping elements (5). The stem can be described by three parameters: width (6), length (7), angle with respect to the base (8), angle of curvature of stem transition to base (9). The base can be described by its width (10) and length (11). Overall fastener geometry has an element width (12) and length (13) and can be rotated (14) and projected (15). (*d*) Examples of different hook geometries obtained by applying key hook design parameters in C that morph the hook geometry: baseline J-shaped hook [66], (i); capped hook [67] results from rotating grip with parameter 14, (ii); ridge hook [71] results from out- of-plane extrusion of the basic J-shaped hook with parameter 15, (iii); J-shaped hook [72] with varied 2D parameters (1–13), (iv); hook [71] with an added gripping element (5), (v); geometrically complex hooks result from varying 2D parameters [73], rotating the grip (14), and extruding out-of- plane (15), (vi); Drawings modified after their cited patents.

from natural fibers or nylon [10,69,119,161,162] and introduced the manufacturing method of cutting woven loop elements to form hooking elements [10,69,119,121,128,161,163,164]. To achieve high strength without the risk of brittleness, hooking elements made of steel have been manufactured using die cutting [146,147], laser cutting [12], and shape deposition [11,15,38]. In fabrication processes such as extrusion, elastic polymers including thermoplastics are utilized, because they maintain their material properties after melting and can solidify into the desired fastener geometry. Thermoplastics are also popular because they are thought to reduce skin irritation of hooking elements [86,95,160], reduce fastener noise [109,165] and perform better under intense heat when made from flame-retardant polymers [104]. For performance under a broader range of extreme temperatures, smart materials have been proposed for several probabilistic fastener designs [13,98,166]. One manufacturing application which has not been utilized for probabilistic mechanical fasteners is 3D printing. Future designs could investigate using additive manufacturing technologies to create novel probabilistic mechanical fasteners from the macrodown to the nano-and submicron scales [167].

3.3 Probabilistic Fastener Traits and Design Trade-Offs. Depending on design choices such as element geometry, material, and method of manufacturing, there are at least eight key traits that vary among probabilistic mechanical fasteners. As seen in Fig. 8, these traits vary and combine in distinct ways across artificial and biological probabilistic mechanical fasteners. For the scoring used in Fig. 8, see Table 4. Here we discuss these traits and the corresponding design trade-offs for probabilistic mechanical fasteners.

3.3.1 Fastener Release Force. The force required to release a mated fastener determines both the strength of attachment and the ease of detachment. In general, individual hooking elements made of engineering materials are stronger than their biological counterparts. The two strongest hooking elements for fasteners reported in the literature are microspines [15] and Metaklett hooks [146] which are both made from steel, see Fig. 9. In addition to material selection, the strength of the attachment can be increased by increasing the friction between fastening elements [171], optimizing element geometry, and increasing the scale of the hooking elements. The downside to increasing the strength of the attachment is that the ease of release is lost, see Fig. 8. Higher force to release could limit applications and potential end-users. Furthermore, increasing the hooking elements' stiffness and strength also increases their potential to damage surfaces they are not designed to mate with, such as human skin and clothing.

3.3.2 Degree of Order and Number of Mating Surfaces. The degree of order in a fastener is described by the spatial

Table 3 Methods for manufacturing and materials for probabilistic mechanical fasteners

Manufacturing method	Material
Die cutting	• Stainless steel 1.421 [146] • thermoplastics [147]
Photonic Professional CT system nanoscribe GmbH	• IP-S photoresist (Nanoscribe GmbH) [14]
Shape deposition manufacturing	• High speed steel [15] • Hardened steel [11,38]
Molding	• Shape memory alloy NiTi [13,98] • Foam [149] • Resin [105,150–152] • Nylon 66 [114] • Thermoplastic [91,103, 106, 108,153]
Extrusion	• Thermoplastics [88,94,97,148,189] • Polypropylene [155] • Polyethylene [155] • Shape memory plastics [156] • Resin [105,157] • Silicones [148,149]
Weaving/knitting	• Thermoplastics [120,159,160] • Nylon 6 [121] • Natural fibers [106]
Casting	• Silicones [148,149] • Polymers [158]
Lamination/embossing	• Thermoplastics [127,142,161]

Note: Since the potential applications of probabilistic fasteners are influenced by material compositions and manufacturing methods, it is beneficial to spend time considering material/manufacturing combinations which result in the desired fastener behaviors. For example, probabilistic fasteners which require strong hooking elements are suited for steel materials and can be manufactured using die cutting or shape deposition. On the other hand, more flexible probabilistic fasteners can be made from a variety of polymers and manufacturing methods.

arrangement and orientations of fastening elements relative to each other and to the engaging surface. Probabilistic mechanical fasteners in industry tend to be more ordered than those found in nature, see Fig. 8. The evolution of burdock seeds hooking to a wide range of animal furs for seed dispersal exemplifies how it is beneficial to have a fastener with a high degree of disorder to reduce the need for attachment precision and increase the likelihood of attachment [18,22,48,49]. Whereas having two patterned and predetermined surfaces limits the available interaction surfaces, it effectively guarantees successful surface mating (see Figs. 2 and 3), because each element in the array is designed to engage with the mating surface [18,22,48,49,169]. For such predetermined fasteners, self-mating surfaces tend to have the most ordered elements while hook-and-loop fasteners are more disordered, as seen in Fig. 8.

3.3.3 Directionality. Most probabilistic mechanical fasteners engage when the hooking and mating elements are brought into close contact; attachment is regardless of the relative motion of each surface with respect to the other, provided that their surfaces are in contact. However, in the new category of directional probabilistic fasteners we review here, the attachment is dependent upon the direction of relative movement and corresponding applied contact force. This directionality is determined by the geometry and relative orientations of the fastening elements, see Fig. 5 for an example. This requires a patterned fastener geometry that repeats across the array, of which the hooking action of each element is reversable and sufficiently aligned across all elements. Directional fasteners based on few hooking elements are found in front-hind wing interlocking mechanisms in insect [47,48,50] and between thousands of hooking elements between the overlapping flight feathers of birds [26], see Fig. 5. To our knowledge, there are currently no engineered directional artificial probabilistic mechanical fasteners. These fasteners have a particularly easy release, see Fig. 8, as disengagement only requires removal of force in the loading direction, or a displacement in any direction other than the attachment direction. Difficulties in designing for directionality include the more constrained microgeometries and alignment precision required across all micro-elements.

3.3.4 Durability. One of the main attributes of probabilistic fasteners is durability, or the ability to repeatably perform for long periods of time under a variety of conditions. However, there are conditions which can be challenging for certain probabilistic fastener designs. Hook-and-loop fasteners, for example, are notorious for failing under conditions where dirt or lint are introduced [172]. While some fastener materials lack durability under very high or low temperatures, smart materials have been shown to improve fastener performance under extreme temperatures [13,98,160]. An area where durability has yet to be thoroughly improved for probabilistic mechanical fasteners is enhancing performance in wet and or chemical environments. For repeatable fastener applications, improved durability is key to increasing fastener lifespan and broadening applications.

3.4 Modelling and Simulation of Probabilistic Mechanical Fasteners. Modelling and simulations of probabilistic mechanical fasteners inform design choices by predicting modes of failure. Probabilistic mechanical fasteners tend to fail in strength or stiffness and can be examined analytically using small stress–strain beam equations. Figure 10 provides an overview of the different failure modes for a hooking element modeled as a curved cantilever beam. Failure in strength has been examined for both hooking and asperity mating elements: hooking elements primarily fail under tensile and shear stress and asperity elements fail when the applied pressure exceeds their ultimate strength [11]. Failures in stiffness for hooking elements include excessive tip rotations and plastic deformations [11]. Whether modelling stiffness or strength of a fastener element, there are several variables which must be identified for the modeling framework including: operating limits

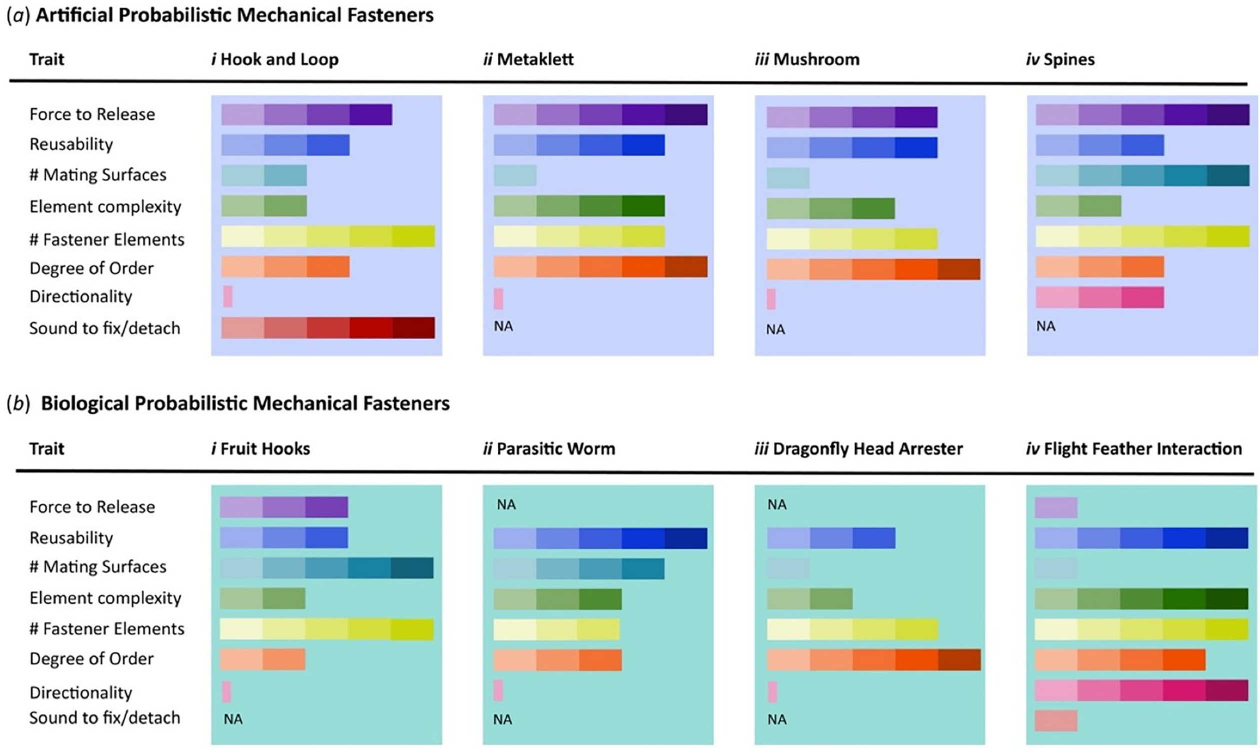

Fig. 8 Traits comparison among artificial and biological probabilistic mechanical fasteners. There is a wide variety of artificial and biological fasteners with structures and materials suited to unique functions. (*a*) In general, artificial fasteners (i)–(iv) are more ordered and have a higher force of detachment compared to biological fasteners. (*b*) Many biological fasteners (i)–(iv) are less ordered so that they can interact with a wider range of surfaces in their environment as seen in seed and fruit hooks [4,10,24,39] and parasitic worms [17]. However, biological fasteners can also be highly specialized to engage with a specific surface, such as the dragonfly head arrester system [21] and microstructures engaging between overlapping flight feathers of many birds, such as Columbia livia (Fig. 5; [25]). There are unique traits that are only found in biological fasteners, which include directionality and associated minimal sound to fasten and detach (although fastener failure can still be as noisy as classical hook-and-loop fasteners). Comparing common fastener traits such as force to release, reusability, and element complexity gives insight in trade-offs between fastener function, structure, and material. Understanding how function, structure, and material determine fastener traits is a key step towards novel designs. A table with the criteria used to score the traits can be found in Table 4.

of key variables (angles for tip rotation, usable asperity slopes, angles of applied load, magnitude of applied load, etc.), material properties such as Young's modulus, and type of applied load (e.g., tensile, shear, bending).

The most readily available tool for multiphysics structural performance simulation is the finite element method (FEM) [13,146,166,173,174]. However, before simulating a probabilistic fastener design, there are several limitations which must be considered. A key limitation is the statistical variation in the microstructure and molecular properties of a single fastener element [175,176]. For general design purposes, these variations can be ignored and bulk material properties and geometries assumed for a quantitative analysis given that the continuum assumptions hold. For smaller scale structures, the outcomes can only be considered qualitative unless validated by experimentation [177–180]. Another simulation challenge for probabilistic fasteners is the long computation time. Probabilistic fasteners are made up of a vast number of elements that fall within a broad scale range from the individual microshaped elements to the macroscale array. This limitation could be resolved by course-graining the fully resolved fastener model to predict macrofastener-level behavior; however, such models have yet to be developed for fastener simulation. We thus consider commonly used analytical continuum and FEM models for (sufficiently large) hooking and mating elements that fail in strength and stiffness.

3.4.1 Modelling Failures in Strength. For probabilistic fastener elements, failures in strength appear as fractures and cracks and can be attributed to stress concentrations exceeding ultimate strength under applied loads. Models for failures in strength of hooking elements are found in Table 5; a visual reference for failure in strength of a cantilever beam is shown in Fig. 10. Hooking elements tend to reach their ultimate strength under tensile and shear loads. Failures from tensile stress have been modelled as cantilever beams where the max stress occurs at the base of the hooking element [11]. A more complicated model which includes the nonlinear behavior of a hook modeled as a curved beam can be used to find the max attachment force [37]. While hooking elements engaging with predetermined loops, self-mating structures, and random environmental surfaces all experience tensile loads, shear loads are more prominent in hooking elements engaging with a random asperity surface. Shear stress occurs at sharp tip of a hooking element as it is pulled across an asperity surface and can cause the tip to break and become increasingly dull [16]. Failures in strength have also been studied in asperity mating elements where max pressure exceeds the ultimate strength and the asperity itself breaks from the mating surface [11].

3.4.2 Modelling Failures in Stiffness. When a hooking element is elongated beyond its operating limit, it fails in stiffness. Relevant stiffness failure models and equations are found in Table 6; a visual reference of examining stiffness failure in a cantilever beam is found in Fig. 10. The failure in stiffness can be plastic or elastic. For elastic failures, there have been several approaches to describe the displacement and rotation of the hook tip at the moment it loses contact with the mating element [11,37,169]. Tip

Table 4 Reference for scoring traits in Fig. 8

Trait	0	1	2	3	4	5
Force to Release	Completely passive	Order at or below 10×10^{-5} N	Order of 10×10^{-4} N	Order of 10×10^{-3}N	Order of 10×10^{-2} N	Order of 10 N
Reusability	One time use before permanent damage	Few uses before permanent damage	All structures prone to damage from repetition	Reusable but has structures prone to damage from Repetition	Many uses with small degree of damage	Many uses with very little damage
# Mating Surfaces	No mating surfaces	One Mating surface	One main mating surface but can interact with other surfaces	Several main mating surfaces but can interact with other surfaces	Interacts with specific randomly encountered surfaces	Interacts with wide variety of randomly encountered surfaces
Element complexity	Stem based fastener elements	j-based fastener elements	Capped fastener elements	Multiple grips on single fastener element	Multiple grips and different orientations of fasteners	Hierarchical fastening elements with different geometries
# Fastener Elements	No individual fastener elements	Very Few fastener elements total	Few fastener elements total	Several fastener elements total	Many fastener elements total	Field of many fastener elements on each mating surface
Degree of Order	No discernable structure or fastening elements	Two fastening surfaces with no set orientations/ geometries	One fastening surface with set geometry	One patterned fastening surface	Two patterned fastening surfaces with some variability	Two Artificially patterned fastening surfaces
Directionality	No directionality	Structures engage under all directions	Structures engage under almost all directions	Structures engage in many directions	Structures engage in up to three directions	Structures designed to only engage in a certain direction
Sound to fix/ detach	No detectable sound	Detectable sound	Detectable and somewhat audible sound	Clearly audible sound	High audible sound	Highest reported sound in literature for probabilistic fasteners

Note: Figure 8 compares several probabilistic fastener traits between biological and artificial designs including: force to release, reusability, # of mating surfaces, element complexity, # of fastener elements, degree of order, directionality, and sound to fix/detach. This table provides the reasoning behind the scoring for each probabilistic fastener trait on a scale of 0 to 5.

rotation of a hooking element has been examined using small stress–strain equations for models of a single curved beam [11] and for two cantilever beams where the stem and base are represented by one beam and the grip is represented by the other [169]. Small stress–strain equations are also used to find the deflection at which the connection between capped mushroom hooks are released under load [169]. Hook rotation and displacement has further been modeled using nonlinear mechanics [39]. This nonlinear model has been applied to the study of fruit hooks [39]. While there are varying levels of complexity in these approaches, the general model for hooking elements is a cantilever beam in bending which is also utilized in FEM simulations for probabilistic mechanical fasteners.

3.4.3 Finite Element Method Simulations. Simulations complement analytical models by examining stress concentrations and deformations throughout the loading process of a hooking element. To approximate the behavior of the hooking element, beam models are used in FEM simulations [13,166]. Material properties can be assumed homogeneous or composite modelling can be used if the material is more complex, as in the case of biomaterials such as cellulose [13,98,181]. Before applying the load, the boundary conditions of the model are defined with a fixed boundary condition at one end and a free end where the load is applied. Stroke, or hook elongation, is measured as the distance from the loading point to the fixed point. Applied load plotted against stress and hook stroke can reveal the points at which the hooking element begins to yield and ultimately fails under a maximum load [13,146]. FEM simulations can also be used to optimize hooking element geometry for a given load using a parameter study [146]. In most cases, the sequence of starting with a joined fastener pair and breaking the connection is sufficient, although behavior for rejoining a broken fastener has also been examined [146]. The results of a simulation or analytical models require validation via experimental testing, especially for micro-and nanoscale fastening elements

3.5 Mechanical Testing of Probabilistic Fasteners. The success of a probabilistic fastener is generally defined by its ability to maintain static attachment under loading and dynamically for application of a load over many cycles. For fasteners and adhesives in general, these tests include peel tests, tensile detachment tests, pull out/pull off tests, single fiber fragmentation tests, torsion tests, and blister tests [182]. The appropriate test is determined by the type of adhesive, fiber orientation, and structure of the fastening elements. For probabilistic mechanical fasteners, tests to evaluate performance include peel tests, friction tests, pull off/pull out tests, noise generation tests, and stress–strain analyses. Descriptions of some of these tests are shown in Fig. 11. When comparing fastener performance test outcomes, the effect of variables such as relative size, strength, and material choice need to be corrected for.

3.5.1 Peel Tests. The peel test is one of the most common tests used to evaluate probabilistic fasteners, because it is their primary method of disengagement. The peel test is performed by applying a force normal to the cross-sectional area of the fastener

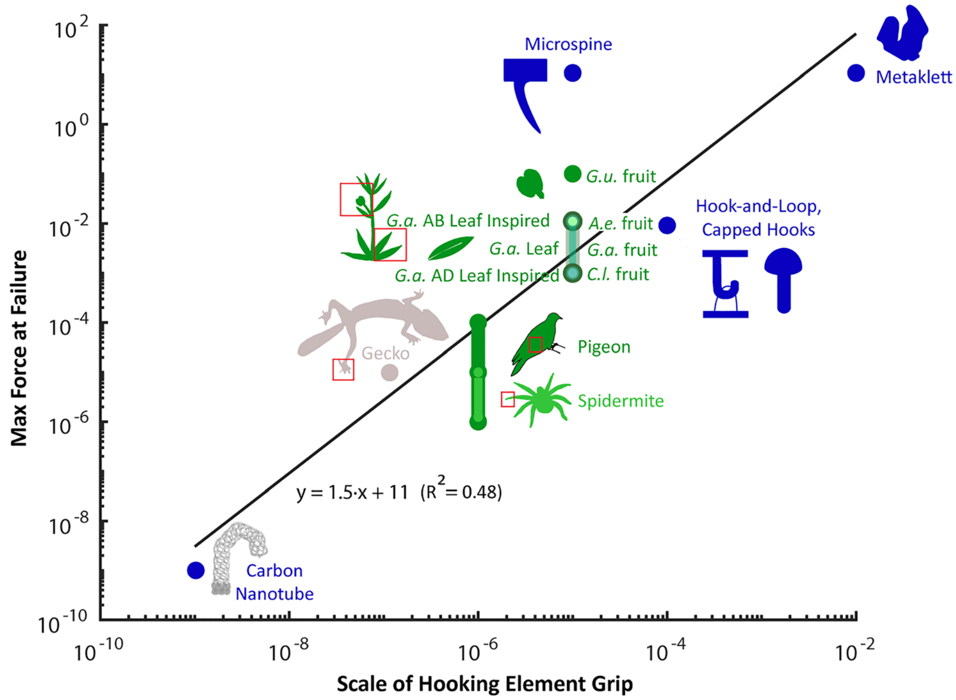

Fig. 9 Reported force at failure for single hooking elements in artificial and biological probabilistic fasteners across seven orders of magnitude in length. This figure presents reported values on the maximal force per hooking element for seven artificial fasteners represented by blue markers and seven biological fasteners represented by green markers. The gecko setae was not included in the linear fit but is shown for reference in gray [3]. Although the Carbon Nanotubes are at a scale where van der Waals forces become a factor [168], they were included in the fit as they are the smallest scale fastener utilizing hooking found in a search of the literature. The four artificial bio-inspired designs include the hook-and-loop [169], microspine [11], and two galium aparine leaf inspired fasteners [14]. The majority of biological data comes from analysis of leaf, seed, and fruit hook fasteners. The weak power law fit is partly due to the microspine outlier which outperforms the scaling law by a significant factor for its scale. The biological avatars were hand drawn. Artificial avatars were modified after and printed with permission from *Sage Publications Inc. Journals* [11], *Trans Tech Publications, LTD* [146], with permission of *Springer* [169], and the *American Physical Society* [170].

and gradually increasing the angle at which the force is applied [169], see Fig. 11 panel (*a*). Measurements of interest for this test include plotting the force versus the peel angle to find the critical angle and plotting the peel strength versus the number of peeling cycles [184]. Variations of the peel test have been developed to examine fastener performance [13,169,182,183].

In the standard peel test, the fastener half with hooking elements is adhered to a piece of tape and peeled from the mating surface, which is fixed to a rigid substrate [169]. The peel force and peel angle are related using Eq. (20) [169] where P is the peel force, b is the tape width, Ga is the energy required to de-adhere a unit area of bond, and θ is the peel angle:

$$\frac{P}{b} - \frac{G_a}{1 - \cos\theta} \tag{20}$$

Another variation is the T peel test, see Fig. 11 panel (*b*), where both the hooking and mating surfaces flex as they are peeled apart [13]. In a shear peel test, see Fig. 11 panel (*c*), a shear force is applied to each mating surface and could potentially be adapted to analyze new directional fasteners [183].

3.5.2 Friction Test. A friction test identifies the engagement of hooking elements with a mating surface. This test is performed by dragging the hooking element surface across the complementary mating surface and measuring the force versus distance [13,24], see Fig. 11 panel (*e*) for a reference. Sudden force peaks reveal instances where hooking elements are engaged with the mating surface and an increase of force is required to disengage the elements. The critical angle up to which friction prevents sliding of the hooked microstructures is the friction angle and can be determined experimentally [13]. This particular test has previously been used to demonstrate the ability of leaf hooks to engage loop elements [24].

3.5.3 Pull Out and Slip Off Tests. The pull out test, see Fig. 11 panel (*d*), is a destructive test which applies a tensile force to individual hooking elements to determine the max force and corresponding displacement at which the elements are removed from their substrate [4,13,24,39,58,98,146]. A general distinction from a peel test is that a pullout test has a rigid substrate while a peel test has a flexible substrate [13]. The hooking elements can also be removed from their natural substrate and glued to a more rigid substrate to examine changes in pull out behavior [39]. Pull out tests have been used to compare pull out force between different species of fruit hooks [4], to confirm capacity of metal hooking elements [146], and to examine contact separation dependence on hooking element morphology [58].

Slip off tests examine the max tensile force at which a hooking element gives way and allows a loop element to be released. The slip off, or unhooking event, is monitored by pulling the fastening elements apart along a prescribed axis line while measuring the pulling force. The pulling force is stopped at the event of unhooking, which is characterized by a sharp drop in the pulling force [98]. Finally, the force at slip off is impacted by the application of tensile forces under different angles at various locations along the hooking element as well as by changes in the morphology of the hooking element [24].

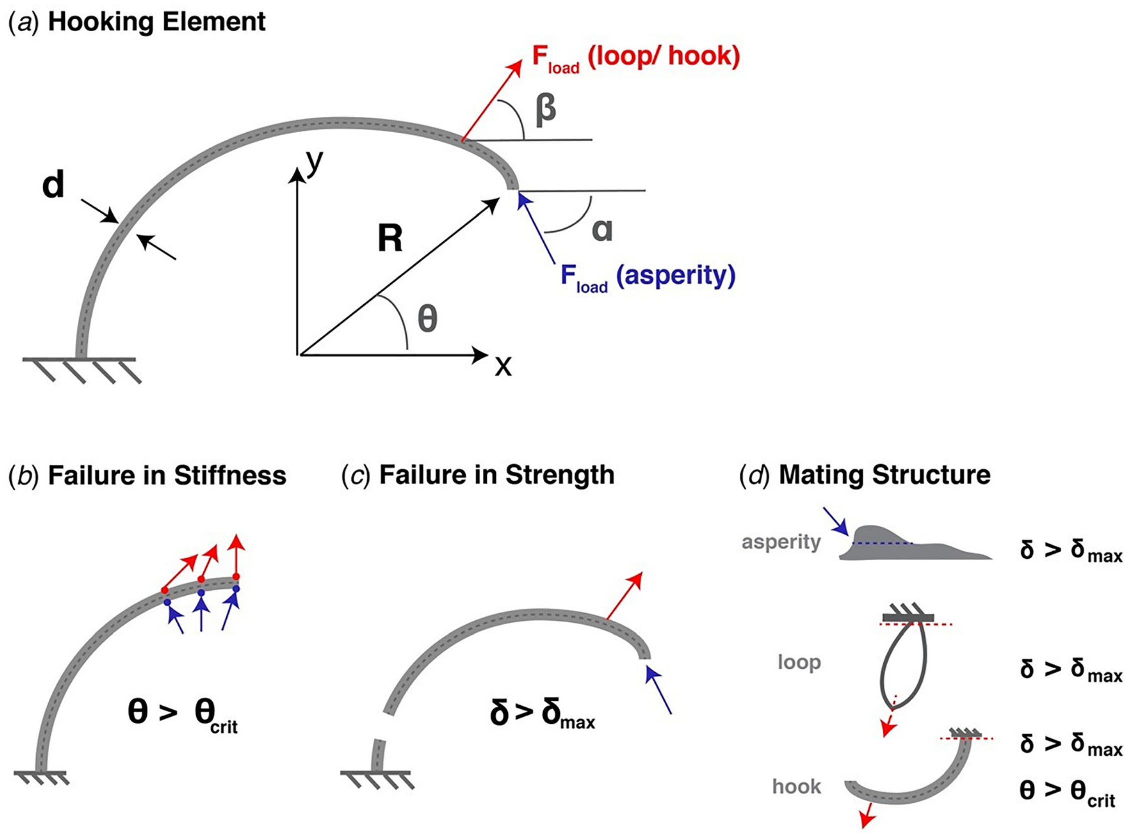

Fig. 10 Determination of hooking element failure modes based on classic cantilever beam models. Cantilever beams are used to examine hooking element failures. (*a*) A cantilever beam model is described with a coordinate reference system, geometric parameters such as radius of curvature and thickness/diameter, and by the applied loads. There are three modes by which a hooking element contact may fail including: (*b*) Failure in stiffness where the hooking element displaces at a critical angle that allows the mating element to slip away. (*c*) Failure in strength where the applied load results in a crack or break when a max stress is reached, causing mating element detachment, and (*d*) failure in the strength or stiffness of a mating structure. Blue indicates loads relevant to a model for a random asperity mating surface (such as bio-inspired spines) and red indicates loads for patterned mating surfaces (such as loop or self-mating surfaces). Drawings modified after and printed with permission from *Sage Publications Inc. Journals* [11].

Table 5 Expressions for failure in strength of hooking and asperity mating elements

Model	Equation	Variables
Cantilever beam [11]	$$\delta_{\max} = \frac{Mc}{I} \quad (12)$$	$\delta_{\max}$: max stress M: moment c: distance from neutral axis I: second moment of area
Shear stress at hook tip [16]	$$F_s = \frac{4F_r}{\pi\left(d(y)^2\right)} \quad (13)$$	F_r: applied load $d(y)$: hook cross-sectional diameter at loading position y
Asperity failure [11]	$$P_{\max} = \frac{3f}{2\pi\alpha^2} \quad (14)$$	$P_{\max}$: max pressure f: normal force applied to hook/asperity contact α: radius of contact patch
Compliant hook [37]	$$F_h = \frac{\left(\frac{\pi}{2} + \varphi\right)\mathrm{EI}}{\pi R^2} \quad (15)$$	F_h: maximum attachment force φ: friction angle between hook and substrate R: hook radius of curvature E: Young's modulus I: second moment of area

Note: One of the failure modes for probabilistic fastener elements is failure in strength for both hooking elements and asperities for the case of a random asperity mating surface. Here we show equations for determining loads which could be used as limiting factors when examining fastener failures in strength. Equations (12), (13), and (15) examine failures in hooking elements under applied loads while Eq. (14) examines asperity failure under loading.

Table 6 Expressions for failure in stiffness of hooking elements

Model	Equation	Variables
Curved beam [11]	$$\alpha = \frac{dU}{dM} = \frac{R^2}{2EI}\left[-2F_y + \left(2F_x + F_y(\pi + 2\beta)\right)\cos(\beta) + \left(-2F_y + F_x\pi + 2F_x\beta\right)\sin(\beta)\right] \quad (16)$$	α: end rotation U: strain energy in the beam M: end moment E: young's modulus I: second moment of area β: angle from the y-axis to the tip of the hook F_x: force component in x direction F_y: force component in y direction
Two cantilever beams [169]	$$\Phi_1 + \Phi_2 + \Phi_3 = \frac{Pw}{EI}\left[h + \frac{w}{2} + \frac{EI}{k}\right] = \varphi + \lambda + \psi \quad (17)$$	Φ_1, Φ_2, Φ_3: rotations at root, tip, and contact point P: applied load E: young's modulus I: second moment of area h: length of stem w: horizontal distance from stem to point of applied load k: rotational stiffness of hook root φ: initial angle from tip to horizontal λ: friction angle between hook and loop surfaces ψ: angle from applied load to shaft of stem
Mushroom hooks [169]	$$\delta = \frac{Ph^2 r_c}{2EI} \quad (18)$$	δ: displacement P: applied force h: height of mushroom stem r_c: radius of mushroom cap E: young's modulus I: second moment of area
Compliant hook [37]	$$\delta(F) = u(F)\sin(v_c(F)) \quad (19)$$	F: applied force $\delta(F)$: vertical displacement $u(F)$: displacement $v_c(F)$: contact angle

Note: Another failure mode for probabilistic fastener elements is failure in stiffness. Understanding limits of stiffness for fastening elements can provide limits for fastener designs. Limits of stiffness are described in Eqs. (16)–(19) in terms of hooking element displacements and rotations. In Eqs. (16) and (17), we reference cantilever beam equations which define rotations of the hooking elements under an applied load. Equation (18) references the special case of displacement in mushroom shaped hooks under applied loads and Eq. (19) examines displacement in a compliant hook.

3.5.4 Noise Generation Spectral Analysis. A noise generation spectral analysis test determines the level of noise generation during fastener detachment. Creating a fastener that is quiet compared to typical hook-and-loop fasteners for everyday use has first responder, police, and military applications [185] as well as increasing auditory comfort. Design solutions to achieve a silent fastener include avoiding a peeling detachment [165] and using shape memory polymers [108]. A spectral analysis of a NiTi hook array and Klettostar Velcro© measured noise generation during a 90-deg peel test and found the NiTi hook array to be quieter [13]. A spectral analysis of an adhesive closure revealed that it was also more silent then the hook-and-loop fastener [186]. However, there remains work to be done in developing more silent probabilistic mechanical fastener. Recently, this test was performed to failure in the newly discovered directional probabilistic fasteners in bird feathers [25]. Bio-inspired design based on the flight feather fastening mechanism (Fig. 5), may facilitate silent fasteners.

3.5.5 Additional Performance Tests and Evaluations. Additional performance tests and evaluations have been developed to examine failures for specific probabilistic mechanical fasteners. For example, damage from repeated cycles on hook-and-loop fasteners can be revealed through imaging [186]. The durability for hook-and-loop fasteners has further been examined by analyzing performance under increasing concentrations of lint [184]. For probabilistic fasteners made of smart materials, stress-strain analyses have examined performance under varying temperatures [166] and under functional fatigue [13]. Functional fatigue tests have also been used to examine probabilistic mechanical fasteners made of steel and include dynamic, quasi-static, and alternating static and dynamic loads [146]. After loading, measurements of the deformed steel hooks can be taken using a tactile contour measurement [146] and the strength of the joining connections can be measured using a cross tension test [146]. The choice of performance test will depend on the geometry, material, and application of the fastener.

3.6 Design Benchmark: Force at Failure for Hooking Elements. To aid in the evaluation of a probabilistic mechanical fastener design, we present a trend between the scale of the hook's grip and the max force per hooking element for a spectrum of biological, artificial, and bio-inspired probabilistic mechanical fasteners. As seen in Fig. 9, the scale of the hook's grip spans from carbon nanohooks [170] at the nm range to Metaklett [146] at the mm range. The associated forces in Fig. 9 vary from nN for carbon nanohooks [170] to the order of 10 N for microspines [15] and Metaklett [146]. Between the microspines and Metaklett, the microspines could be considered higher performing based on the smaller scale of its gripping element sustaining similar magnitudes of force. The bio-inspired hooking elements shown in Fig. 9 are microspines [15], Galium aparine inspired hooks [14], and the burdock seed inspired hook-and-loop fastener [169]. When comparing a design with the scale and max force of existing probabilistic mechanical fasteners, it is important to also consider factors such as material, mode of engagement (e.g., directionality), and the structure of the mating surface. Finally, a caution for examining hooks at the nm level is that van der Waals forces play a role at this scale [168].

Another potential metric that could be used to evaluate and compare fasteners is examining the load at which fastener

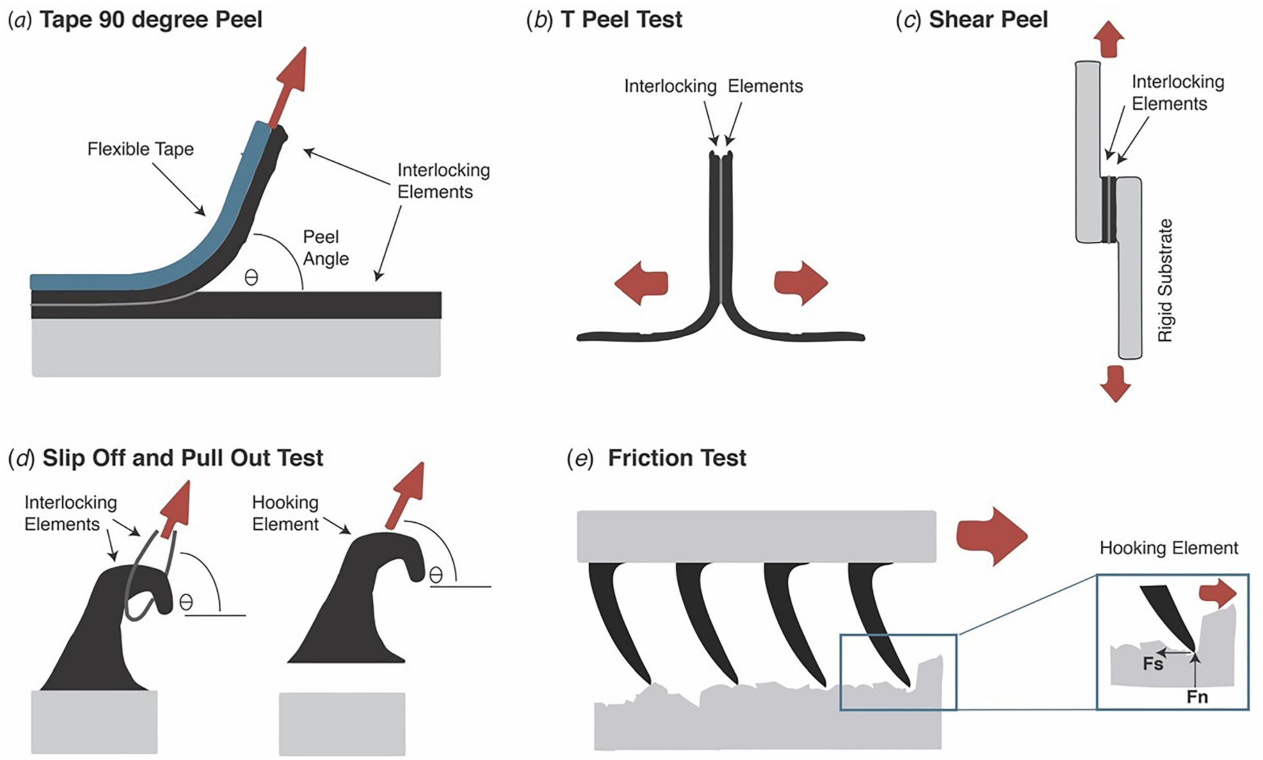

Fig. 11 Common mechanical tests to evaluate the performance of probabilistic fasteners. (*a*) 90-degree peel test applies a force normal to the cross- sectional area and increases the angle of application until all fastener elements have disengaged [169]. Note the force angle starts at 0-degrees and gradually increases to 90-degrees in this test. (*b*) The *T* peel test applies force to both mating surfaces and is not constrained by a rigid substrate [13,183]. (*c*) Shear peel test is applicable to directional fasteners, pulling the fastener elements in shear until they reach a critical force and disengage [183]. (*d*) The slip off test examines the force and angle at which a loop element loses connection with the hooking element and while the pull-out test examines the force and angle at which a hooking element is pulled out of its substrate [4,13,24,49,54,58,98,146]. (*e*) In the friction test, the hooking element is pulled across a surface with a random asperity distribution. A rise in the loading force pulling the hook across the surface identifies the instance when that the hooking element engages with an asperity and resists the pull of the loading force [11,13,24]. Drawings modified after [183] and printed with permission from and *The Royal Society of Chemistry*. Drawings modified and printed with permission from *Sage Publications Inc. Journals* [11] and with permission of *Springer* [169].

elements develop cracks. While the literature has focused on fastening element failure due to slip or catastrophic failure in strength, more insight into fastener design could be gained by studying the loads at which cracks first appear and propagate in fastener elements. Fracture energy has been studied in biological composites such as shells, bones, and enamel, whose elementary units, mineralized fibrils, are structured to optimize stiffness and toughness [187]. The complex hierarchy of biological composites maximizes adhesion as well as flaw tolerance in the overall composite and in the individual fibers [59,187]. However, there is a limit at which levels of hierarchy increase adhesion strength and protect from crack formation, as described in a gecko inspired model based on van der Waals forces [59]. As more hierarchical levels of fibers are added, eventually the model reaches a point where fiber fracture becomes the dominant failure mode of the system level. The limiting hierarchical level is found by determining the fibril level at which the maximum tensile stress that the cracked fibers can sustain is greater than the adhesion strength of the system as shown by the following equation [59]:

$$\sigma_n^{\max} = \sqrt{\frac{E_f \Gamma_f}{R_n}} * \sqrt{\frac{\pi * \frac{R_n}{2a}}{g * \left(\frac{a}{R_n}\right)}} \tag{21}$$

Here E_f is the Young's modulus of the fiber, R_n is the radius of the fiber at level n, a is the crack radius, g is a geometric parameter, and Γ_f is the fracture energy of the fiber. The limiting factor is $\sigma_n^{\max} > \mathrm{Sn}$, where Sn is the adhesion strength [59]. To our knowledge, there is currently no artificial or bio-inspired hierarchical fastener. Using the limiting factor, $\sigma_n^{\max}$ as described in Eq. (21), and the principle of a limiting hierarchical level, more complex hierarchical fastener designs may be developed.

4 Applications and Opportunities

4.1 Current Areas of Application and Opportunities. Probabilistic mechanical fasteners are particularly useful for applications which benefit from secure, repeatable, flexible attachments that require little skill. These versatile traits make probabilistic mechanical fasteners appropriate for a variety of applications. However, when choosing a fastener for a specific application, it is helpful to first compare it to other attachment technologies and determine which technology best fulfills the application requirements. In Table 7, we present a comparison of different attachment technologies to clarify when a probabilistic mechanical fastener may be appropriate over other technologies [188]. As seen in Fig. 12, fields where the probabilistic mechanical fasteners particularly flourish include medicine, apparel, storage and transportation, and robotics.

In the medical field, probabilistic fasteners are used to provide comfortable attachments for splints [164] and disposable garments [71,78,136,190–192]. An additional medical application examined using an array of hooks from a hook-and-loop fastener for the bristles of a toothbrush [193]. In medical research, a

Table 7 Comparison of attachment technologies and suggested areas of application (adapted with minor changes from [204])

Technology	Benefits	Limitations	Suggested applications
Suction	– Strong, repeatable attachments on smooth surfaces	– High level of noise during release of suction cups – Requires a smooth surface to operate efficiently – For robotics, a pump mechanism is needed to remove and engage suction cups for locomotion applications	– Static attachments on smooth surfaces
Electro-adhesion	– Can attach to variety of surfaces, including both smooth and rough surfaces – Requires little energy to power to release and engage the adhesion – Quiet release and attachment mechanism – Tolerates dust and cleaning	– Requires a continuous power input to maintain an attachment	– Robotics climbing and locomotion
Wet Adhesion	– Strong attachment on variety of surfaces – Quiet release and attachment mechanism	– High-energy cost to release the attachment – Needs an adequate supply of adhesive to draw from when forming a new attachment – May leave adhesive residue on the surface	– Prolonged or indefinite static attachments on surfaces which allow for adhesive residue
Dry Adhesion	– Little energy input needed to maintain attachments – Quiet release and attachment mechanism	– Energy to release an attachment can be high – Peeling release mechanism can cause damage to individual fastening elements – Attachment is limited or impossible on surfaces which are dusty, wet, or made of certain plastics	– Temporary static attachments and climbing on clean surfaces with a degree of roughness
Claws	– Little energy input needed to maintain attachments – Impervious to dust or moisture on a variety of surfaces – Very high attachment strength	– Unable to climb smooth surfaces – May cause puncture, scratches, or other damage to surface	– High strength grasping of surfaces which allow for damage
Probabilistic mechanical fasteners	– Reversible, repeatable, and durable attachments – Reliable: secure attachment achieved without a high level of precision or expert skill – Versatile: can be designed for high or low attachment forces, can attach to custom or random mating surfaces, may be quiet or loud, and can secure and release attachments through different mechanisms such as directional or peeling attachments	– Surface asperities are necessary for climbing applications – Hooking elements may damage mating surface. – Release mechanism, such as a peeling detachment, may damage hooking elements – Attachment is inhibited by dust and or moisture	– Consumer friendly applications – Indefinite static attachment – Repeatable and durable attachments – Directional attachments

Note: In order to clarify the merit of probabilistic mechanical fasteners, we present a comparison between different attachment technologies. When designing a new attachment technology, it may be useful to consult this table and confirm which attachment technology is best suited for the desired application based on its benefits and limitations.

biocompatible hook-and-loop type fastener was used to attach a micro-electrode array to a nerve [173]. An area with potential opportunity for new directional probabilistic fasteners includes applications for individuals who suffer from arthritis and weak grip strength, because the directionality makes them substantially easier to release.

The textile industry employs probabilistic fasteners in footwear [194] and garments [110] for their easy adjustment and release. Probabilistic fasteners can be adjusted in a variety of step sizes while typical textile fasteners like buttons are limited by "discrete adjustment steps" [22]. The concept of easy release has further been applied in combat uniform design where hook-and-loop fasteners were shown to reduce tourniquet removal time compared to buttoned fasteners [195]. Design opportunities for textiles could include reducing snag of textiles on the hooking elements [196], comfort of fastener elements on the skin [86,95,163] and ease of attachment or release.

In storage and transportation, probabilistic mechanical fasteners are utilized to secure bulky objects. Self-mating fasteners with both hooking and mating surfaces on a single strap are the most common design used in these applications [99,197–201]. However, custom designed fasteners with separate fastening surfaces

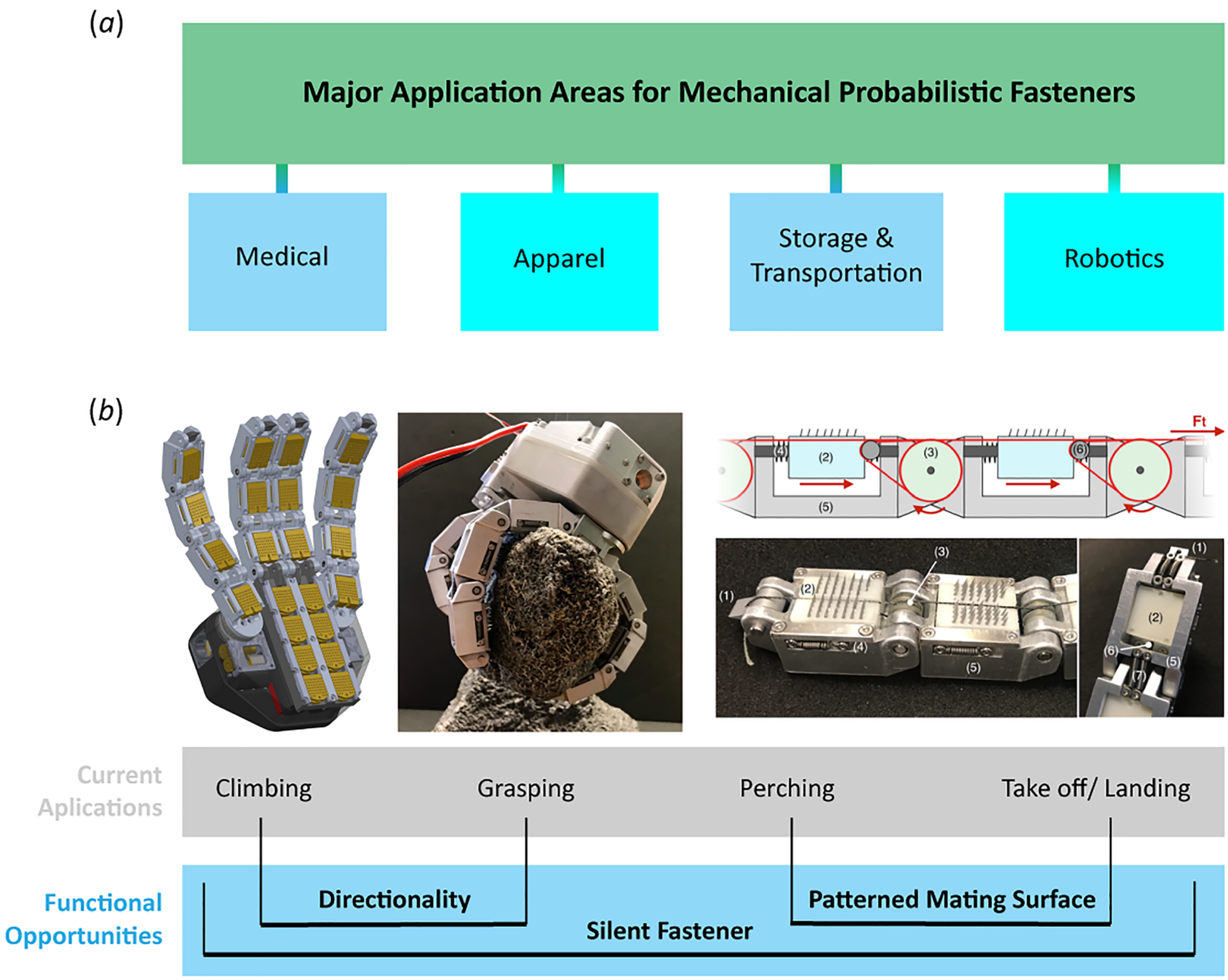

Fig. 12 Applications of mechanical probabilistic fasteners and opportunities to implement underutilized characteristics. The strong, repeatable, and reconfigurable attachments of probabilistic fasteners make them relevant to a wide variety of applications. (*a*) The major application areas for mechanical probabilistic fasteners are the medical, apparel, storage and transportation, and robotics fields. In each of these (and other) fields there are opportunities to improve current fastener performance and to introduce underutilized characteristics to innovate the fastener design. (*b*) Taking the field of robotics as an example, key applications including climbing, grasping, perching, and take off/landing all utilize the traits of high probability, strong, and repeatable probabilistic mechanical fasteners that require minimal kinematic interaction precision. Adding a novel characteristic to these probabilistic mechanical fasteners, such as directionality could advance climbing and grasping performance, while designing patterned mating surfaces for perching and takeoff/landing could provide more stability. Finally, introducing silent fastening into robotics could further improve the customer experience during human- robot interactions and enhance the overall stealth of a robot's locomotion in covert operations. Images were adapted and printed with permission from *ASME* [189].

have been examined for securing products within the fastener system. This is done by forming fastener elements around the outline of the product so that it can be sandwiched between the fastener surfaces [202].

In robotics, probabilistic fasteners have been employed for grasping objects and random mating surfaces in their operating environment. Spines inspired by the hooks on insect feet have been used on to grasp objects [16] including ones in low gravity environments [203] as well as for latching onto stochastic surfaces in climbing applications [11,32]. A Galium aparine leaf hook inspired fastener has also been investigated in robotic grasping applications [14]. Currently, most robotics applications have one custom designed hook-based fastener that interacts with mating surfaces featuring the typical degree of randomness encountered in the environment. The design of patterned hook and mating surfaces for locking devices is one area where robotics may benefit from probabilistic mechanical fasteners. Locking devices aid robots in energy management as well as reconfiguration [204]. Some of the ideal characteristics of locking devices in robotics have been identified to include: high locking force, short switching time, light weight, compact design, low energy consumption, adjustable locking directions, capability to lock in any position, and unlocking under a load [204]. Given that many of these characteristics are found in probabilistic fasteners, we identify locking devices as an area of opportunity for these fasteners. Specific probabilistic mechanical fasteners traits which could be incorporated into robotics applications are described in Fig. 12.

Both gecko-inspired technologies based on van der Waals forces [196,197] and electro-adhesion [188,205–207] have also been used for robotics applications, most notably for locomotion [207] and climbing across surfaces [188]. There are some noteworthy differences in these technologies compared to probabilistic mechanical fasteners. Gecko-inspired technologies based on dry adhesion share similar characteristics with some probabilistic mechanical fasteners: they disengage with a peel mechanism and their effectiveness is reduced by the presence of dust [188];

a. Applied Physics

A. Physical	B. Chemical	C. Mechanical
1. Electirc Current 2. Magnetic Field 3. Welding	1. Van der Waals Forces 2. Adhesive Bonds 3. Hydrogen Bonds	1. Bolting 2. Threading 3. Stitching 4. Lashing 5. Crimping 6. Tying

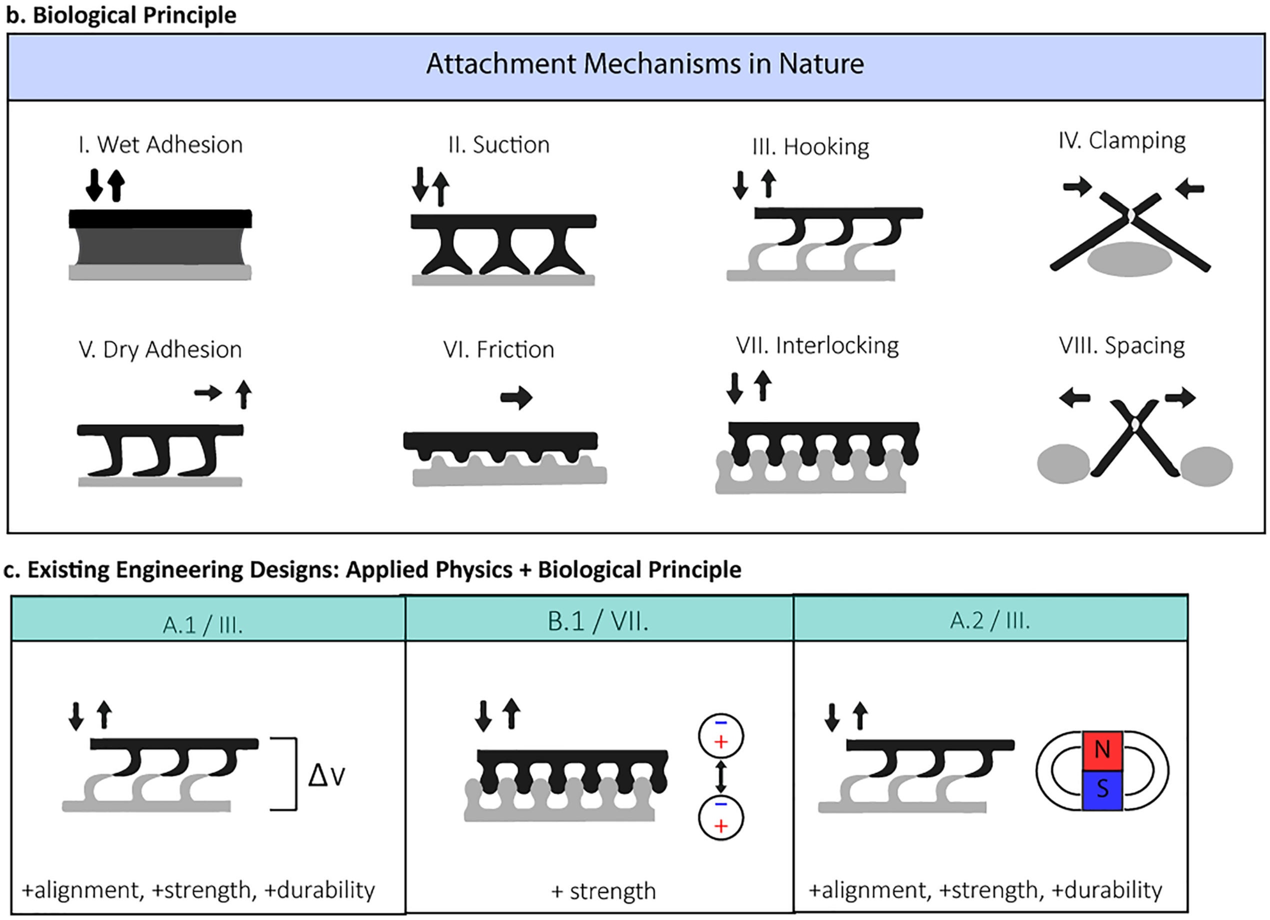

Fig. 13 Enhancing probabilistic mechanical fasteners with multiple attachment principles. Combining different physical and biological principles can lead to the creation of new fasteners with improved performance. (*a*) A wide range of applied physics attachment principles have been harnessed across artificial fasteners based on Physical, A, Chemical, B, and Mechanical, C, interaction, respectively. (*b*) The described biological principles for attachment include wet adhesion, I, suction, II, hooking, III, clamping, IV, dry adhesion, V, friction, VI, interlocking, VII, and spacing, VIII; based on [19]. Our literature review revealed three innovative engineering designs which combine applied physics (*a*) and biological (*b*) principles. In column c(A.1 and III), a new active probabilistic fastener combines probabilistic hooking (b(III)) with electric current (a(A.1)) to improve the alignment of mating surfaces, fastening strength, and durability. Column c(B.1 and VII) combines Van der Walls forces (a(B.1)) with interlocking (b(VII)) to improve fastener strength. Finally, column c(A.2 and III) actively combines probabilistic hooking (b(III)) with a magnetic field (a(A.2)) to improve alignment of mating surfaces, fastening strength, and durability. Improved durability is made possible by controlling the peel-off detachment via active magnetic field (or electric current) switching [98,209–211]. This integration of applied physics with biological principles expands the opportunity for fastener innovation. Drawing modified after [19] and printed with permission from *the Royal Society*.

however, the "van der Waals forces effectively ensure that the fastener is always 'on' which can increase the energy required to disengage an attachment" [188]. Electro-adhesion on the other hand, has "the benefit of low energy consumption as the attachment can easily be controlled to turn on or off" [188,206]. The electro-adhesive is controlled by switching voltages on/off to secure and release an attachment. Inspired by inchworms and caterpillars, electro-adhesion has been used on actuator feet to produce omnidirectional creeping in soft robots [207]. Additional benefits are that electro-adhesion provides dust tolerance, quiet operation, fast response, and lack of dependence on surface asperities which suits this technology for robotic locomotion [188,206]. Depending on the application, electro-adhesion or van der Waals-based designs may be preferred over probabilistic mechanical fasteners. In order to capture the strengths of each of these technologies, a robot could potentially be designed with interchangeable parts which each utilize a different attachment technology. Another possibility is to combine multiple attachment technologies into a single device to gain a more robust attachment with a broader operating range. For example, combining electrostatic adhesion with a gecko inspired setae structure has been investigated for attachment applications [205]. The potential applications afforded by combining attachment technologies is an exciting possibility inspired by biological examples of organisms integrating different attachment mechanisms to more robustly adhere to a wider range of surfaces [22,208].

4.2 Multi-Attachment Strategy to Inspire Novel Fastener Designs. Nature has developed specialized fasteners that utilize multiple attachment principles to enhance their performance. For example, some larvae found in rivers use wet adhesion combined with mechanical hooking to secure themselves against water flow [22]. We believe that drawing from nature's strategy of enhancing fastener performance with multiple attachment principles will inspire new fastener designs. To this end, we present a strategy, as seen in Fig. 13, of combining attachment principles found in both manufacturing (Applied Physics) and nature (Biological Principles, see Fig. 1). Taking a combination of two principles from the total of 20 attachment strategies and using the C(20,2) for the combination formula $C(n,r) = n!/(r!(n-r)!)$ reveals 190 possible designs. A search of the literature revealed that of these 190 designs, there are only three multi-attachment fasteners which have been proposed. These include combining electric and magnetic fields with hooking elements [98,209–211] additional mechanical hardware with hook and loop fasteners [212], and Van der Walls fasteners with interlocking elements [213]. Including these multiple attachment principles is proposed to increase strength by improving fastener alignment and to increase durability in hook/hook-and-loop fasteners by removing the need for a peeling detachment.

5 Conclusion

Probabilistic mechanical fasteners are secure, reversible, and repeatable attachment devices which require little skill to operate. While examples of different mechanisms for these fasteners are found in nature, most artificial designs are variations of the hook-and-loop fastener inspired by Galium aparine seed hooks. In total, there are only four known bio-inspired mechanical probabilistic fasteners [10,11,14–17,37]. However, we have shown that there is opportunity to create a wide range of new designs by drawing upon the characteristics of fasteners found in nature, such as directionality, silent fastening, and hierarchical organization. The functionality of fasteners can be further diversified and enhanced by integrating existing physical interaction principles in the design. In summary, the combination of the bio-inspired design framework and the established and new approaches help guide solving shortcomings in existing fasteners and open pathways to new applications.

Acknowledgment

We would like to acknowledge Mark Cutkosky for helpful suggestions, Laura Matloff for comments on our outline, Teresa Feo for feather morphological expertise, and William Roderick for many insights that helped layout the review.

Funding Data

- This review was supported by AFOSR BRI Award No. FA9550-16-1-0182 with special thanks to B. L. Lee for leading the program (Funder ID: 10.13039/100000181).
- This review was additionally supported by AFOSR DESI Award No. FA9550-18-1-0525. L. J. was supported by an NSF GRFP award and D. L. by NSF Early Faculty Career Development (CAREER) Award No. 1552419 (Funder ID: 10.13039/100000001).

References

[1] Messler, R. W., 2006, *Integral Mechanical Attachment: A Resurgence of the Oldest Method of Joining*, Elsevier, Amsterdam, The Netherlands.

[2] Zhao, Y., Wu, Y., Wang, L., Zhang, M., Chen, X., Liu, M., Fan, J., Liu, J., Zhou, F., and Wang, Z., 2017, "Bio-Inspired Reversible Underwater Adhesive," Nat. Commun., **8**(1), p. 2218.

[3] Autumn, K., Liang, Y. A., Hsieh, S. T., Zesch, W., Chan, W. P., Kenny, T. W., Fearing, R., and Full, R. J., 2000, "Adhesive Force of a Single Gecko Foot-Hair," Nature, **405**(6787), pp. 681–685.

[4] Gorb, E., and Gorb, S., 2002, "Contact Separation Force of the Fruit Burrs in Four Plant Species Adapted to Dispersal by Mechanical Interlocking," Plant Physiol. Biochem., **40**(4), pp. 373–381.

[5] Baik, S., Kim, D. W., Park, Y., Lee, T.-J., Ho Bhang, S., and Pang, C., 2017, "A Wet-Tolerant Adhesive Patch Inspired by Protuberances in Suction Cups of Octopi," Nature, **546**(7658), pp. 396–400.

[6] Brodoceanu, D., Bauer, C. T., Kroner, E., Arzt, E., and Kraus, T., 2016, "Hierarchical Bioinspired Adhesive Surfaces-a Review," Bioinspiration Biomimetics, **11**(5), p. 051001.

[7] O'Rorke, R. D., Steele, T. W. J., and Taylor, H. K., 2016, "Bioinspired Fibrillar Adhesives: A Review of Analytical Models and Experimental Evidence for Adhesion Enhancement by Surface Patterns," J. Adhes. Sci. Technol., **30**(4), pp. 362–391.

[8] Sun, J., and Bhushan, B., 2019, "Nanomanufacturing of Bioinspired Surfaces," Tribol. Int., **129**, pp. 67–74.

[9] Yason, L., Krahn, J., and Menon, C., 2016, "Bioinspired Dry Adhesive Materials and Their Application in Robotics: A Review," J. Bionic Eng., **13**(2), pp. 181–199.

[10] de Mestral, G., 1955, Velvet Type Fabric and Method of Producing Same, Patent No. 2,717,437.

[11] Asbeck, A. T., Sangbae, K., R Cutkosky, M., R Provancher, W., and Lanzetta, M., 2006, "Scaling Hard Vertical Surfaces With Compliant Microspine Arrays," Int. J. Rob. Res., **25**(12), pp. 1165–1179.

[12] Hippmann, S., Hein, C., and Hoffmann, H., 2008, "Correlation Between the Adhesive Tensile Strength and the Engagement Grade of Crosswise Oriented Nonwovens of Metal Hook and Loop Fasteners," Prod. Eng., **2**(4), pp. 395–400.

[13] Vokoun, D., Sedlák, P., Frost, M., Pilch, J., Majtás, D., and Šittner, P., 2011, "Velcro-Like Fasteners Based on NiTi Micro-Hook Arrays," Smart Mater. Struct., **20**(8), p. 085027.

[14] Fiorello, I., Tricinci, O., and Mishra, A. K., 2012, "Artificial System Inspired by Climbing Mechanism of Galium Aparine Fabricated via 3D Laser Lithography," *Biomimetic and Biohybrid Systems*, pp. 168–178.

[15] Jiang, H., Wang, S., and Cutkosky, M. R., 2018, "Stochastic Models of Compliant Spine Arrays for Rough Surface Grasping," Int. J. Rob. Res., **37**(7), pp. 669–687.

[16] Wang, S., Jiang, H., and Cutkosky, M. R., 2017, "Design and Modeling of Linearly- Constrained Compliant Spines for Human-Scale Locomotion on Rocky Surfaces," Int. J. Rob. Res., **36**(9), pp. 985–999.

[17] Spina, G. L., Stefanini, C., Menciassi, A., and Dario, P., 2005, "A Novel Technological Process for Fabricating Micro-Tips for Biomimetic Adhesion," J. Micromech. Microeng., **15**(8), pp. 1576–1587.

[18] Gorb, S. N., and Popov, V. L., 2002, "Probabilistic Fasteners With Parabolic Elements: Biological System, Artificial Model and Theoretical Considerations," Philos. Trans. R. Soc. A, **360**(1791), pp. 211–225.

[19] Gorb, S. N., 2008, "Biological Attachment Devices: Exploring Nature's Diversity for Biomimetics," Philos. Trans. R. Soc. A, **366**(1870), pp. 1557–1574.

[20] Gavin, H., Jon, W., and Barnes, W. P. J., 1991, "Adhesion and Detachment of the Toe Pads of Tree Frogs," J. Exp. Biol., **155**, pp. 103–125.

[21] Gorb, S. N., 1999, "Evolution of the Dragonfy Head-Arresting System," Proc. Biol. Sci., **266**(1418), pp. 525–535.

[22] Natchtigall, W., 1974, *Biological Mechanisms of Attachment: The Comparative Morphology and Bioengineering of Organs for Linkage, Suction, and Adhesion*, Springer, Berlin.

[23] Wilker, J. J., 2017, "Materials Science: How to Suck Like an Octopus," Nature, **546**(7658), pp. 358–359.

[24] Bauer, G., Klein, M. C., Gorb, S. N., Speck, T., Voigt, D., and Gallenmüller, F., 2011, "Always on the Bright Side: The Climbing Mechanism of Galium Aparine," Proc. R. Soc. B: Biol. Sci., **278**(1715), pp. 2233–2239.

[25] Matloff, L. Y., Chang, E., Feo, T. J., Jeffries, L., Stowers, A. K., Thomson, C., and Lentink, D., 2020, "How Flight Feathers Stick Together to Form a Continuous Morphing Wing," Science, **367**(6475), pp. 293–297.

[26] Kovalev, A., Filippov, A. E., and Gorb, S. N., 2014, "Unzipping Bird Feathers," J. R. Soc. Interface, **11**(92), p. 20130988.

[27] Roderick, W. R. T., Cutkosky, M. R., and Lentink, D., 2017, "Touchdown to Take-Off: At the Interface of Flight and Surface Locomotion," Interface Focus, **7**(1), p. 20160094.

[28] Budiansky, B., Evans, A. G., and Hutchinson, J. W., 1995, "Fiber-Matrix Debonding Effects on Cracking in Aligned Fiber Ceramic Composites," Int. J. Solid Struct., **32**(3–4), pp. 315–328.
[29] Budiansky, B., Hutchinson, J. W., and Evans, A. G., 1986, "Matrix Fracture in Fiber-Reinforced Ceramics," J. Mech. Phys. Solids, **34**(2), pp. 167–189.
[30] Curtin, W. A., 1991, "Theory of Mechanical Properties of Ceramic-Matrix Composites," J. Am. Ceram. Soc., **74**(11), pp. 2837–45.
[31] Curtin, W., 1998, "Stochastic Damage Evolution and Failure in Fiber-Reinforced Composites," Adv. Appl. Mech., **36**, pp. 163–253.
[32] Harlow, D. G., and Phoenix, S. L., 1982, "Probability Distributions for the Strength of Fibrous Materials Under Local Load Sharing I: Two-Level Failure and Edge Effects," Adv. Appl. Probab., **14**(1), pp. 68–94.
[33] Rossoll, A., Moser, B., and Mortensen, A., 2012, "Tensile Strength of Axially Loaded Unidirectional Nextel 610TM Reinforced Aluminium: A Case Study in Local Load Sharing Between Randomly Distributed Fibres," Compos. Part A: Appl. Sci. Manuf., **43**(1), pp. 129–137.
[34] Schechner, Z., 1984, "A Load-Sharing Model: The Linear Breakdown Rule," Nav. Res. Logistics Q., **31**(1), pp. 137–144.
[35] Siddique, S., and Volovoi, V., 2014, "Failure Mechanisms of Load-Sharing Complex Systems," Phys. Rev. E - Stat., Nonlinear, Soft Matter Phys., **89**(1), pp. 1–7.
[36] Swolfs, Y., McMeeking, R. M., Rajan, V. P., Zok, F. W., Verpoest, I., and Gorbatikh, L., 2015, "Global Load-Sharing Model for Unidirectional Hybrid Fibre-Reinforced Composites," J. Mech. Phys. Solids, **84**, pp. 380–394.
[37] Pugno, N. M., 2007, "Velcro® Nonlinear Mechanics," Appl. Phys. Lett., **90**(12), p. 121918.
[38] Asbeck, A. T., and Cutkosky, M. R., 2012, "Designing Compliant Spine Mechanisms for Climbing," ASME J. Mech. Rob., **4**(3), p. 031007.
[39] Chen, Q., Gorb, S. N., Gorb, E., and Pugno, N., 2013, "Mechanics of Plant Fruit Hooks," J. R. Soc. Interface, **10**(81), p. 20120913.
[40] Gorb, E. V., Popov, V. L., and Gorb, S. N., 2002, "Natural Hook-and-Loop Fasteners: Anatomy, Mechanical Properties, and Attachment Force of the Jointed Hooks of the Galium Aparine Fruit," Design and Nature, **3**, pp. 151–160.
[41] Howell, L. L., 2013, "Compliant Mechanisms," *21st Century Kinematics*, J. Michael McCarthy, (ed.), Springer, London, pp. 189–217.
[42] Yu, Y.-Q., Zhu, S.-K., Xu, Q.-P., and Zhou, P., 2016, "A Novel Model of Large Deflection Beams With Combined End Loads in Compliant Mechanisms," Precis. Eng., **43**, pp. 395–405.
[43] Howell, L. L., and Midha, A., 1995, "Parametric Deflection Approximations for End-Loaded, Large-Deflection Beams in Compliant Mechanisms," ASME J. Mech. Des., **117**(1), pp. 156–165.
[44] Saxena, A., and Kramer, S. N., 1998, "A Simple and Accurate Method for Determining Large Deflections in Compliant Mechanisms Subjected to End Forces and Moments," ASME J. Mech. Des., **120**(3), pp. 392–400.
[45] Dejean, A., Leroy, C., Corbara, B., Roux, O., Céréghino, R., Orivel, J., and Boulay, R., 2010, "Arboreal Ants Use the '"Velcroh Principle"' to Capture Very Large Prey," PLoS One, **5**(6), p. e11331.
[46] Whitney, H. M., Lars, C., Bruce, T. J. A., and Glover, B. J., 2009, "Conical Epidermal Cells Allow Bees to Grip Flowers and Increase Foraging Efficiency," Curr. Biol., **19**(11), pp. 948–953.
[47] Pang, C., Kwak, M. K., Lee, C., Jeong, H. E., Bae, W. G., and Suh, K. Y., 2012, "Nano Meets Beetles From Wing to Tiptoe: Versatile Tools for Smart and Reversible Adhesions," Nano Tod., **7**(6), pp. 496–513.
[48] Gorb, S. N., 2002, "Structural Design and Biomechanics of Friction-Based Releasable Attachment Devices in Insects," Integr. Comp. Biol., **42**(6), pp. 1127–1139.
[49] Gorb, S. N., 2002, "Miniature Attachment Systems: Exploring Biological Design Principles," Comparing Des. Nat. Sci. Eng., pp. 123–133.
[50] Gorb, S., 2001, *Attachment Devices of Insect Cuticle*, Springer, Berlin.
[51] Sick, V. H., 1937, "Morphologisch-Funktionelle Untersuchungen Fiber Die Feinstruktur Der Vogelfeder. Heft Die Feinstruktur Der Vogelfeder. Deren Meiste Gerade Den Bau Des Fertig Ausgebildeten Organs Zum Gegenstand Haben. So Wurde Dieses Thema Auch Nicht Direkt in an- Grif," J. Ornithol., **1937**(2), pp. 206–372.
[52] Oehme, V. H., 1963, "Flight and Wings of Star and Blackbird, Part 1: Biophysics of Flight," Biologisches Zentralblatt, **82**(4), pp. 414–454.
[53] Rutschke, V. E., 1965, "Uber Den Silberschimmer Auf Den Schwungfedem Yon Seeschwalben," J Ornithol., **106**, pp. 307–312.
[54] Prum, R. O., 1999, "Development and Evolutionary Origin of Feathers," J. Exp. Zool., **285**(4), pp. 291–306.
[55] Yu, M., Wu, P., Widelitz, R. B., and Chuong, C. M., 2002, "The Morphogenesis of Feathers," Nature, **420**(6913), pp. 308–312.
[56] Lucas, A. M., and Stettenheim, P. R., 1972, "Avian Anatomy: Integument—Parts I and II," Agricultural Handbook (362), U.S. Government Printing Office, Washington, DC.
[57] Sullivan, T. N., Chon, M., Ramachandramoorthy, R., Roenbeck, M. R., Hung, T.-T., Espinosa, H. D., and Meyers, M. A., 2017, "Reversible Attachment With Tailored Permeability: The Feather Vane and Bioinspired Designs," Adv. Funct. Mater., **27**(39), p. 1702954.
[58] Zhang, F., Jiang, L., and Wang, S., 2018, "Repairable Cascaded Slide-Lock System Endows Bird Feathers With Tear-Resistance and Superdurability," Proc. Natl. Acad. Sci. United States Am., **115**(40), pp. 10046–10051.
[59] Yao, H., and Gao, H., 2006, "Mechanics of Robust and Releasable Adhesion in Biology: Bottom-Up Designed Hierarchical Structures of Gecko," J. Mech. Phys. Solids, **54**(6), pp. 1120–1146.
[60] Suprun, E., Sahin, O., Stewart, R., and Panuwatwanich, K., 2017, "Dealing With Complexity: A Holistic Participatory Systems Approach for Improving Construction Innovation Performance," 35th International Conference of the System Dynamics Society, Cambridge, MA, July 16–20, pp. 1–14.
[61] Eroglu, A. K., Erden, Z., and Erden, A., 2011, "Bioinspired Conceptual Design (BICD) Approach for Hybrid Bioinspired Robot Design Process," IEEE International Conference on Mechatronics (ICM)—Proceedings, Istanbul, Turkey, Apr. 13–15, pp. 905–910.
[62] Qin, Z., Dimas, L., Adler, D., Bratzel, G., and Buehler, M. J., 2014, "Biological Materials by Design," J. Phys. Condens. Matter, **26**(7), p. 073101.
[63] Filippov, A. E., Popov, V. L., and Gorb, S. N., 2015, "The Functional Significance of Density and Distribution of Outgrowths on Co-Opted Contact Pairs in Biological Arresting Systems," Philos. Trans. R. Soc. B, **370**(1661), p. 20140032.
[64] Seale, M., Cummins, C., Viola, I. M., Mastropaolo, E., and Nakayama, N., 2018, "Design Principles of Hair-Like Structures as Biological Machines," J. R. Soc. Interface, **15**(142), p. 20180206.
[65] Efremova, N. V., Woltman, G. R., McDaniel, M. L., Quincy, R. B., III, Kraft, N., and Eby, T. A., 2010, "Mechanical Fastener," Patent No. 7,725,992 B2.
[66] Ottaviani, R. A., Ulincy, J. C., and Golden, M. A., 2005, "Magnetorheological Nanocomposite Elastomer for Releasable Attachment Applications," Patent No. 6,877,193 B2.
[67] Noel, J. R., and Scripps, C. L., 1991, "Loop Fastening Material for Fastening Device and Method of Making Same," Patent No. 5,032,122.
[68] Kurtz, W. L. J., Van Benschoten, B., Tachauer, E. S., Pierce, J. E., and Neeb, A. J., 2004, "Fastener Product With Multiple Engagement Angles," Patent No. 2004/0261232 A1.
[69] Ito, M., and Ogihara, T., 1985, "Hooked Fabric Fastener Tape," Patent No. 4,541,154.
[70] Provost, G. A., 1998, "Hook and Loop Fastening and the Like," Patent No. 5,755,016.
[71] Ausen, R. W., Unruh, W. C., Miller, P., and Seth, J., 2007, "Heat Treated Profile Extruded Hook," Patent No. 7185401 B2.
[72] Gallant, C. M., 2007, "Fastener Product," Patent No. 7,225,510 B2.
[73] Clarner, M. A., Provost, G. A., and Huber, W. L., 2004, "Hook and Loop Fastener," US Patent No. 2004/0031130A1
[74] Gallant, C. M., Clarner, M. A., and Dowd, C., 2013, "Arrays of Fastener Elements," Patent No.8,448,305 B2.
[75] Yamada, Y., 1990, "Hook Element for Surface Fasteners," Patent No. 4912819.
[76] Kennedy, W. J., and Rocha, G. F., 1994, "Hook Design for a Hook and Loop Fastener," Patent No. 5339499.
[77] Shepard, W. H., and Provost, G., 2013, "Hook-Engageable Fastener Sheets, and Methods and Articles of Manufacture," US Patent No. 8,500,940 B2.
[78] Provost, G. A., 1999, "Fastener Component With Flexible Fastener Members," Patent No. 5887320.
[79] Lacey, T. G., Provost, G. A., Filion, S. M., Kaparis, E., Dowd, C., Van Stumpf, J., Condon, M. J., Pollard, S. W., Jens, S. C., and Grulke, P. E., 2000, "Molding Fastening Hooks Other Devices," Patent No. 6,163,939
[80] Miller, P., and Melbye, W. L., 2000, "J Hook-Type Strip for a Mechanical Fastener," Patent No. 6,054,091.
[81] Armela, L. P., Sanchez, J., Clune, W., Davis, J., Gallant, C. M., Clarner, M. A., and Huber, W. L., 2003, "Fasteners Engageable With Loops of Nonwoven Fabrics and With Other Open Structures, and Methods and Machines for Making Fasteners," Patent No. 2003/0106188 A1.
[82] Vanbenschoten, B. J., Gallant, C. M., Sepanik, H. Z., and Tremblay, H. S., 2005, "Direct Hook Engagement," Patent No. 6,904,649 B2.
[83] Vanbenschoten, B. J. E. S., Tachauer, W. L., Kurtz, JR, P. A., Dandurand, W. P., Clune, A. J., Neeb, J. E., Pierce, R. J., Schmidt, and R. W., Tanzer, 2005, "Coextruded Hook Fasteners," US Patent No. US2005/0060849 A1.
[84] Tuman, S. J., Seth, J., Lindquist, T. J., Ista, T. K., and Ausen, R., 2006, "Hook Fastener and Method of Making," Patent No. 7,014,906 B2.
[85] Seth, J., and Ausen, R. W., 2006, "Net Structure and Method of Making," Patent No. 7,048,984 B2.
[86] Martin, T. R., Neeb, A. J., Schmidt, R. J., Vanbenschoten, B. J., Tremblay, H., Gallant, C. M., Filion, S. M., Buzzell, K. G., and Parshley, J. K., 2007, "Skin Friendly Fastener Component," Patent No. 7,162,780 B2.
[87] Cheng, C.-W. A., 2012, "Hook of Hook-and-Loop Fastener," Patent No. D658,044 S.
[88] Murasaki, R., and Minato, T., 2009, "Hook Fastener Structures," Patent No. 7493,676 B2.
[89] Harvey, A. C., Ribich, W. A., Marinaccio, P. J., and Sawaf, B. E., 1987, "Separable Fastening Device," Patent No. 4,709,453.
[90] Zoromski, P. K., Schmidt, R. J., Feldt, M.-P. Y. V., Nortman, B. K., and Long, A. M., 2003, "Male Fasteners With Angled Projections," Patent No. 6,588,073 B1.
[91] Parellada, L., and Sanchez, J., 2004, "Fasteners and Methods of Making Fasteners," US Patent No. US6,708.378 B2.
[92] Golden, M. A., Ulincy, J. C., Browne, A. L., Johnson, N. L., Barvosa-Carter, W., Stanford, T. B., and Momoda, L. A., 2006, "Releasable Fastener Systems and Process," Patent No. 7,013,536 B2.
[93] Cheng, C.-W. A., 2011, "Hook Structure and Injection Molded Hook Strap Including the Same," Patent No. 2011/0258819 A1.
[94] Marche, T., Blanc, O., Medina, N. L. R., Looney, M. T., and Horn, T. A., 2015, "Hook Fastener," Patent No. 2015/0074956 A1.
[95] Provost, G. A., 2000, "Molded Hook Member for a Touch Fastener," Patent No. 6,163,939.

[96] Provost, G. A., Condon, M. J., Leak, A. T., S Roslansky, A., and Serbiak, P. J., 2003, "Hook Fasteners and Methods of Manufacture," Patent No. 6,526,633 B2.
[97] Tachauer, E. S., 2004, "Active Fasteners," US Patent No. US 2004/0088835 A1.
[98] Vokoun, D., Majtás, D., Frost, M., Sedlák, P., and Šittner, P., 2009, "Shape Memory Hooks Employed in Fasteners," J. Mater. Eng. Perform., **18**(5–6), pp. 706–710.
[99] Miller, P., Melbye, W. L., Nestegard, S. K., Wood, L. E., Lindseth, M. D., and Bychinski, D. A., 1998, "Mushroom Type Hook Strip for a Mechanical Fastener," Patent No. 5845375.
[100] Kampfer, R. D., 2000, "Method for Forming Headed Stem Mechanical Fasteners," Patent No. 6,132,660.
[101] Melbye, W. L., Nestegard, S. K., Wood, L. E., Lindseth, M. D., and Bychinski, D. A., 2005, "Method for Making a Mushroom-Type Hook Strip for a Mechanical Fastener," Patent No. US 2005/0039313 A1.
[102] Hanschen, T. P., Ausen, R. W., and Kopecky, W. J., 2015, "Structured Surface With Multiple-Post Caps and Method of Making the Same," Patent No. 8,973,225 B2.
[103] Pearson, R. C., 1965, "Separable Fastener," Patent No. 3,192,589.
[104] Kobe, J. J., 1997, "Flame Retardant Fastener and Method for Making the Same," Patent No. 5,691,021.
[105] Arsenault, C. M., Hargrett, B. T., Kobe, J. J., and Levitt, L., 2000, "Mechanical Fastener," Patent No. 6,076,238.
[106] Rhode, W., 2000, "Hook and Loop Fastener," Patent No. 6,096,667.
[107] West, D. W., 2009, "Microhook Fastener Apparatus," Patent No. US 2009/0126165 A1.
[108] Kirby, B. C., Cable, K. M., Havens, T. E., and Hermiller, J. M., 2011, "Quiet Release Shape Memory Polymer Fasteners," Patent No. 2011/0265292 A1.
[109] Cheng, S. M., 2013, "Mushroom-Type Hook Strap for Mechanical Fasteners," Patent No. 8,609,218 B2.
[110] Moskowitz, D., 2012, "Releasable Securement Device," Patent No. US 2012/0260401 A1.
[111] Tuman, S. J., Seidel, D. L., and Levitt, L., 2001, "Web Having Discrete Stem Regions," Patent No. US 2001/0016245 A1.
[112] Allan, R. M., 1994, "Connector Apparatus With Nesting Ridges," Patent No. 5,345,659.
[113] Clune, W., 1999, "Fastener Members and Apparatus for Their Fabrication," Patent No. 5,884,374.
[114] Tolan, N. J., Clarner, M. A., McDougall, W. B. S., Cote, N. A., Kingsford, H. A., Erickson, P. R., and Dowd, C., 2011, "Low Profile Touch Fastener," Patent No. 8,082,637 B2.
[115] Provost, G. A., and Rocha, G. F., 1991, "Hook for Hook and Loop Fasteners," Patent No. 4984339.
[116] Peake, W. L., III, Spillane, R. T., McCartney, P. D., and Huebner, P. R., 1995, "Loop-Type Textile Fastener Fabric, Method of Producing Same and Process of Treating Same," Patent No. 5,407,722.
[117] Morishita, K., 2012, "Female Part of Hook and Loop Fastener," Patent No. US 2012/0010588 A1.
[118] Baldauf, G., and Homoelle, D., 2013, "Loop Tape for Hook-and-Loop Fastener," Patent No. US 8,347.466 B2.
[119] Naimer, J., 1964, "Separable Fastening Fabrics," Patent No. 3,138,8412.
[120] Kingsford, H. A., and Wang, D.-S., 2004, "Woven Fastener Products," Patent No. US 2004/0166282 A1
[121] Wang, D.-S., and Godlewski, D. E., 2004, "Woven Hook and Loop Fastening," Patent No. US 6,728,998 B2
[122] Wang, D.-S., 2003, "Woven Hook and Loop Fastening," Patent No. US 6,546,603 B1.
[123] Goulait, D. J. K., and Carstens, J. E., 1995, "Loop Fastening Material for Fastening Device and Method of Making Same," Patent No. 5,380,313.
[124] Jackson, W. W., Diaz, M. S., and Garrett, L. J., Jr 1997, "Creped Nonwoven Laminate Loop Fastening Material for Mechanical Fastening Systems," Patent No. 5,614,281.
[125] Billarant, J.-P., 1998, "Laminated Assembly Constituted by a Warp or Weft-Knitted Loop Fabric Adhered Flat on a Support, and Its Manufacturing Method," Patent No. 5,736,214.
[126] Seth, J., and Rogers, J. J., 1999, "Soft Loop Laminate and Method of Making," Patent No. 5,888,607.
[127] Kennedy, W. J., Provost, G. A., and Rocha, G. F., 2004, "Laminated Hook Fastener," Patent No. US 6,737,147 B2.
[128] Becker, D. L., Tochacek, M., and Hansen, P. E., 1990, "Sheet Material Used to Form Portions of Fasteners," Patent No. 4,931,343
[129] Goulait, D. J. K., 1995, "Multi-Layer Female Component for Refastenable Fastening Device and Method of Making the Same," Patent No. 5,407,439.
[130] Dinger, R., Wiegand, J., and Fendt, A., 1997, "Formable Heat-Stabilizable Textile Loop Pile Material," Patent No. 5,654,067.
[131] Jackson, B. M., 1998, "Loop Fastening Material," Patent No. 5,830,298.
[132] McCormack, A. L., Haffner, W. B., and Jackson, W. W., 1999, "Breathable Barrier Composite Useful as an Ideal Loop Fastener Component," Patent No. 5,997.981.
[133] Lawless, B. J., 1999, "Needle Punch Nonwoven Component for Refastenable Fastening Device," Patent No. 5,891,547.
[134] Sheffield, W. F., Barry, J. L., and Slama, D. F., 1999, "Loop Material for Engagement With Hooking Stems," Patent No. 5,962,102.
[135] Martin, T. R., 2004, "Loop Fastening Component Made From Thermally Retracted Materials," Patent No. US 6,756,327 B2.
[136] Filion, S. M., and Schmidt, R. J., 2004, "Varying the Loop Engageability of Fastener Element Arrays," Patent No. US 6,671,935 B2.
[137] Shepard, W. H., and Provost, G. A., 2004, "Loop Materials for Touch Fastening," Patent No. US 2004/0163221A1.
[138] Ducauchuis, J.-P., 2010, "Film Comprising Individual Anchored Filaments," Patent No. US 7,727,611 B2.
[139] Wood, L. E., and Gorman, M. R., 2013, "Corruagted Loop for a Hook and Loop Fastener," Patent No. US D695,097 S.
[140] Chou 2014, "Fastening Fabric Structure," Patent No. US 8,656,564 B2.
[141] Provost, G. A. L., "Hook for Hook and Loop Fasteners," Patent No. 5,315,740.
[142] Ausen, R. W., and Seth, J., 2006, "Reinforced Hook Web," Patent No. 7,067,185 B2.
[143] Provost, G. A., Clarner, M. A., and Kraus, D. P., 2009, "Hook Fastener Components and Methods of Their Manufacture," Patent No. 7,516,524 B2.
[144] Kurtz, W. L., Jr, VanBenschoten, B. J., Tachauer, E. S., Labrecque, M., and Dowd, C., 2006, "Fastener Element and Methods of Manufacture," Patent No. 6,996,880 B2.
[145] Higashinaka, Y., 1993, "Mixed Hook/Loop Separable Fastener and Process for Its Production," Patent No. 5,231,738.
[146] Hoffmann, H., Hein, C., Hong, S., and So, H., 2007, "Metaklett—A Metal Cocklebur," Key Eng. Mater., **344**(344), pp. 677–684.
[147] Banfield, D. L., Roch, G. F., Jacobs, M. I., and Kenney, R. B., 1999, "Die Cut Mold-In," Patent No. 5,922436.
[148] Galkiewicz, R. K., Clarke, G. M., W Ausen, R., and Spiewak, B. E., 2000, "Self-Mating Reclosable Mechanical Fastener," Patent No. US 6,367,128 B1.
[149] Cina, M., Voight, P. J., and Chan, M. W., 2012, "Mold-in Touch Fastening Product," Patent No. US 9,034,452 B2.
[150] Janzen, D. L., K K Line, P. J., and Voight, 2004, "Fasteners," Patent No. US 7,141,283 B2.
[151] Tolan, N. J., Clarner, M. A., McDougall, W. B. S., Cote, N. A., Kingsford, H. A., Erickson, P. R., and Dowd, C., 2003, "Low Profile Touch Fastener," Patent No. US 8,082,637 B2.
[152] Armela, L. P., Sanchez, J., Clune, W., Davis, J., Gallant, C. M., Spezzafero, M., Clarner, M. A., Huber, W. L., Kraus, D. P., Jr, Provost, G. A., Kingsford, H. A., and Labrecque, M., 2004, "Methods of Making Fastener Products," Patent No. US7,727,440 B2.
[153] Martin, T. R., Neeb, A. J., and Schmidt, R. J., 2003, "Hook and Loop Fastener Having an Increased Coefficient of Friction," Patent No. 6,489,004 B1.
[154] Long, A. M., E Huntoon, A., Roocks, L. A., Lord, P. R., and Shaw, G. A., 1997, "Mechanical Fastening System With Grip Tab," Patent No. 5,624,429.
[155] Aultterson, C. S., 2010, "Reclosable Fastener Riser/Spacer, and Methods of Constructing and Utilizing Same," Patent No. US 7,909,393 B2.
[156] Schulte, A., 2001, "Hook-and-Loop Fastener Produced From a Shape Memory Plastic Material," Patent No. US 2004/0033336 A1.
[157] Levitt, L., Kampfer, R. D., Delmore, M. D., Kranpe, S. E., Berg, B. T., Sipinen, A. J., Napierala, M. E., and Thalacker, V. P., 2002, " Elastic Fastener," Patent No. US 6,489,003 B1.
[158] Erb, G. H., and Bead, S. E., 1989, "Method for Making a Hermaphordite Hook and Loop Fasteners," Patent No. 4,999,067.
[159] Cheng, A., 2014, "Method of Manufacturing a Hook Member of a Hook-and-Loop Fastener and a Hook Member Manufactured by the Method," Patent No. 2014/0075724 A1.
[160] Goulait, D. J. K., and Thomas, D. A., 1995, "Non-Abrasive Skin Friendly Mechanical Fastening System," Patent No. 5,392,498.
[161] Nishiyama, H., Takao, H., and Kurobe, K., 1984, "Method and Apparatus for Manufacturing a Hooked Fastener Part for Hook-and-Loop Fasteners," Patent No. 4429441.
[162] Erb, G. H., 1986, "Multiple Hook Fastener Media and Method and System for Making," Patent No. 4,615,084.
[163] Ishihara, M., 2001, "Surface Fastener Made of Fiber and Method for Manufacturing the Same," Patent No. 6,202,264 B1.
[164] Kingsford, H. A., Isabelle, H., Provost, G. A., and Shepard, W. H., 2012, "Medical Wraps," Patent No. 8,231,816 B2.
[165] Cates, M. H., Jr., and Farris, A. F., III, 2015, "Silent Hook and Loop Fastener System," Patent No. US 9,003,615 B1.
[166] Frost, M., Sedlák, P., Sippola, M., and Šittner, P., 2010, "Thermomechanical Model for NiTi Shape Memory Wires," Smart Mater. Struct., **19**(9), p. 094010.
[167] Clune, W., and Provost, G. A., 2000, "Forming Continuous Fastener Material," US Patent No. 6,640,348 B1.
[168] Qu, L., Dai, L., Stone, M., Xia, Z., and Wang, Z. L., 2008, "Carbon Nanotube Arrays With Strong Shear Binding-On and Normal Lifting-Off," Science, **322**(5899), pp. 238–242.
[169] Williams, J. A., Davies, S. G., and Frazer, S., 2007, "The Peeling of Flexible Probabilistic Fasteners," Tribol. Lett., **26**(3), pp. 213–222.
[170] Berber, S., Kwon, K, Y., and Tománek, D., 2003, "Bonding and Energy Dissipation in a Nanohook Assembly," Phys. Rev. Lett., **91**(16), pp. 1–4.
[171] Martin, T. R., Neeb, A. J., and Schmidt, R. J., 2002, "Hook & Loop Fastener Having an Increased Coefficient of Friction," Patent No. US 6,645,600 B2.
[172] Röhrig, M., 2014, *Fabrication and Analysis of Bio-Inspired Smart Surfaces*, KIT Scientific Publishing, Karlsruhe, Germany.
[173] Seki, Y. Yamagiwa, S., Morikawa, Y., Sawahata, H., Numano, R., Ishida, M., and Kawano, T., 2017, "Hook and Loop Microfastener: Flexible Microelectrodes Tied to a Nerve," Proceedings of the IEEE International Conference on Micro Electro Mechanical Systems (MEMS), Las Vegas, NV, Jan. 22–26, pp. 117–120.

[174] Hart, A. H. C., Koizumi, R., Hamel, J., Owuor, P. S., Ito, Y., Ozden, S., Bhowmick, S., Syed Amanulla, S. A., Tsafack, T., Keyshar, K., Mital, R., Hurst, J., Vajtai, R., Tiwary, C. S., and Ajayan, P. M., 2017, "Velcro-Inspired SiC Fuzzy Fibers for Aerospace Applications," ACS Appl. Mater. Interfaces, **9**(15), pp. 13742–13750.
[175] Knauss, W. G., Chasiotis, I., and Huang, Y., 2003, "Mechanical Measurements at the Micron and Nanometer Scales," Mech. Mater., **35**(3–6), pp. 217–231.
[176] Chasiotis, I., Cho, S. W., Friedman, T. A., and Sullivan, J. P., 2003, "Young's Modulus, Poisson's Ratio, and Nanoscale Deformation Fields of MEMS Materials," MRS Online Proc. Libr., **795**, pp. 461–466.
[177] Uchic, M. D., and Dimiduk, D. M., 2005, "A Methodology to Investigate Size Scale Effects in Crystalline Plasticity Using Uniaxial Compression Testing," Mater. Sci. Eng.: A400, **400–401**, pp. 268–278.
[178] Pantano, M. F., Espinosa, H. D., and Pagnotta, L., 2012, "Mechanical Characterization of Materials at Small Length Scales," J. Mech. Sci. Technol., **26**(2), pp. 545–561.
[179] Tajik, A., and Jahed, H., 2012, "Standalone Tensile Testing of Thin Film Materials for MEMS/NEMS Applications," Microelectromech. Syst. Devices, **28**.
[180] Li, X., and Wei, C., 2005, "Optical Full-Field Technique for Measuring Deformation on Micromechanical Components," Third International Conference on Experimental Mechanics and Third Conference of the Asian Committee on Experimental Mechanics, Vol. 5852. International Society for Optics and Photonics.
[181] Saunders, B. E., 2016, "Microdesign Using Frictional, Hooked, Attachment Mechanisms: A Biomimetic Study of Natural Attachment Mechanisms—Part 3," Rob. Biomimetics, **3**(1), p. 4.
[182] Skeist, I., 1990, *Handbook of Adhesives, 3rd Addition*, Springer, New York.
[183] Heinzmann, C., Weder, C., and de Espinosa, L. M., 2016, "Supramolecular Polymer Adhesives: Advanced Materials Inspired by Nature," R. Soc. Chem., **45**(2), pp. 342–358.
[184] Taylor, A. R., Johnson, N. A. G., and Dowdell, B., 1992, "Influence of Ageing and Lint Accumulation on the Fastening Strength of Hook and Loop Fasteners," Textile Res. J., **62**(12), pp. 766–770.
[185] Tucker, J. C., 2018, "Velcro® New Unidirectional HTH 719 Quiet Closure for Military, Police, and Hunters," John C. Tucker Co., Fort Worth, TX, accessed Nov. 15, 2018, https://jctucker.com/velcros-new-unidirectional-hth-719-quiet-closure-for-military-police-and-hunters-2/
[186] King, D. R., Bartlett, M. D., Nalbach, M., Irschick, D. J., and Crosby, A. J., 2017, "High Strength Reversible Adhesive Closures," J. Polym. Sci., Part B, **55**(23), pp. 1783–1790.
[187] Guo, X., and Gao, H., 2006, "Bio-Inspired Material Design and Optimization," Solid Mech. Appl., **137**, pp. 439–453.
[188] Prahlad, H. R., Pelrine, S., Stanford, J., Marlow, R., and Kornbluh, 2008, "Electroadhesive Robots – Wall Climbing Robots Enabled by a Novel, Robust, and Electrically Controllable Adhesion Technology," IEEE International Conference on Robotics and Automation, Pasadena, CA, May 19–23, pp. 3028–3033.
[189] Wang, S., Jiang, H., Huh, T. M., Sun, D., Ruotolo, W., Miller, M., Roderick, W. R. T., Stuart, H. S., and Cutkosky, M. R., 2019, "Spinyhand: Contact Load Sharing for a Human-Scale Climbing Robot," ASME J. Mech. Rob., **11**(3), p. 031009.
[190] McDaniel, M. L., Efremova, N., Pierce, J. E., Yu, L., Van Benschoten, B., Kurtz, W. L., JR,., and Tachauer, E. S., 2008, "Refastenable Absorbent Garment," Patent No. 7.444,722 B2.
[191] Burnes, A. S., and McCormack, A. L., 1998, "Compressively Resilient Loop Structure for Hook and Loop Fastener Systems," Patent No. 5,707,707.
[192] LaFortune, J. M., and LeMahieu, L. K., 1997, "Absorbent Article Having an Improved Mechanical Fastening System," Patent No. 5,669,901.
[193] Ojha, S. K., Javdekar, S. B., and Dhir, S., 2015, "Comparative Evaluation of Enamel Abrasivity by Toothbrush and Velcro: An In Vitro Scanning Electron Microscope Study," J. Indian Soc. Periodontol., **19**(3), p. 263.124X.156873.
[194] Provost, G., and Ouellette, M. C., 1987, "Self-Engaging Separable Fastener," Patent No. 4,654,246.
[195] Higgs, A. R., Maughon, M. J., Ruland, R. T., and Reade, M. C., 2016, "Effect of Uniform Design on the Speed of Combat Tourniquet Application: A Simulation Study," Mil. Med., **181**(8), pp. 753–755.
[196] Schreiner, D. N., 1997, "Retractable Hook and Loop Fastener," Patent No. 5,930,875.
[197] Schriefer, T. D., and Stanfield, E. A., 2004, "Flexible Bundling and Labeling Device," Patent No. US2004/0058121A1.
[198] Cheng, S.-M., 2015, "Fastening Strap and Manufacturing Method Thereof," Patent No. US 9,027,211 B2.
[199] Daniels, J., 1987, "Laminated Fastening Strap," Patent No. 4,643,932.
[200] Romanko, W. R., Trans, H. N., W Ausen, R., Larson, C. L., Unruh, W. C., Mills, M. W., and Mody, K. C., 2002, "High Strength, Flexible, Light Weight Hook and Loop Bundling Straps," Patent No. US 6,484,371 B1.
[201] Shepard, W. H., and Clune, W. P., 2014, "Composite Hook and Loop Fasteners, Methods of Their Manufacture, and Products Containg Them," Patent No. 8,778,243 B2.
[202] Altomare, G. C., 2016, "Aparatus and Method of Embedding Articles Within Reclosable Fastener Systems," Patent No. 2016/0331086 A1.
[203] Jiang, H., 2017, "A Robotic Device Using Gecko-Inspired Adhesives Can Grasp and Manipulate Large Objects in Microgravity," Sci. Rob., **2**(7).
[204] Plooij, M., Mathijssen, G., Cherelle, P., Lefeber, D., and Vanderborght, B., 2015, "Lock Your Robot: A Review of Locking Devices in Robotics," IEEE Rob. Autom. Mag., **22**(1), pp. 106–117.
[205] Koh, K. H., Sreekumar, M., and Ponnambala, S. G., 2014, "Experimental Investigation of the Effect of the Driving Voltage of an Electroadhesion Actuator," Materials, **7**(7), pp. 4963–4981.
[206] Cao, C., Sun, X., Fang, Y., Qin, Q.-H., Yu, A., and Feng, X.-Q., 2016, "Theoretical Model and Design of Electroadhesive Pad With Interdigitated Electrodes," Mater. Des., **89**, pp. 485–491.
[207] Chen, S., Cao, Y., Sarparast, M., Yuan, H., Dong, L., Tan, X., and Cao, C., 2020, "Soft Crawling Robotics: Design, Actuation, and Locomotion," Adv. Mater. Technol., **5**(2), p. 1900837.
[208] Chen, Y., Meng, J., Gu, Z., Wan, X., Jiang, L., and Wang, S., 2020, "Bioinspired Multiscale Wet Adhesive Surfaces: Structures and Controlled Adhesion," Adv. Funct. Mater., **30**(5), p. 1905287.
[209] Kenney, R. B., Routhier, B. J., and Jacobs, M. I., 2001, "Forming Fastener Components of Multiple Streams of Resin," Patent No. US 2001/0038161 A1.
[210] Browne, A. L. N. L., Johnson, C. S., and Namuduri, 2004, "Electrostatically Releasable Fastening System and Method of Use," Patent No. US 2004/0074067 A1.
[211] Joo, H. G., Jang, Y. H., and Choi, H. S., 2014, "Electrical Contact Resistance for a Conductive Velcro System," Tribol. Int., **80**, pp. 115–121.
[212] NASA Tech Brief. 1970, "Quick-Release Hook-and-Loop Fastener," US Patent No. US4864698A.
[213] Keshavarzi, S., Mescheder, U., and Reinecke, H., 2016, "Room Temperature Si – Si Direct Bonding Technique Using Velcro-Like Surfaces," J. Microelectromech. Syst., **25**(2), pp. 371–379.